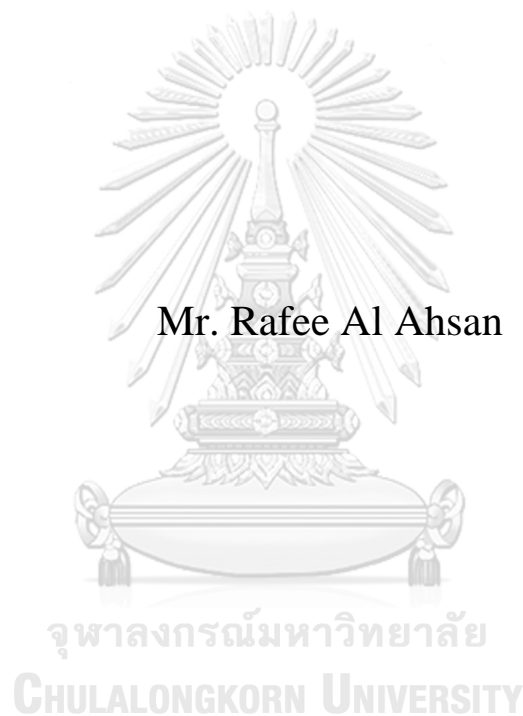


Simplified Tone Reservation-Based Techniques for Peak-to-Average Power Ratio Reduction of Orthogonal Frequency Division Multiplexing Signals



A Thesis Submitted in Partial Fulfillment of the Requirements  
for the Degree of Master of Engineering in Electrical Engineering  
Department of Electrical Engineering  
FACULTY OF ENGINEERING  
Chulalongkorn University  
Academic Year 2021  
Copyright of Chulalongkorn University

เทคนิคการสำรวจโทนอนอย่างง่ายสำหรับการลดค่าอัตราส่วนระหว่างค่ายอดและค่าเฉลี่ยกำลังงานขอ  
งสัญญาณการมัลติเพล็กซ์แบบแบ่งความถี่ตั้งฉาก



วิทยานิพนธ์นี้เป็นส่วนหนึ่งของการศึกษาตามหลักสูตรปริญญาวิศวกรรมศาสตรมหาบัณฑิต  
สาขาวิชาวิศวกรรมไฟฟ้า ภาควิชาวิศวกรรมไฟฟ้า  
คณะวิศวกรรมศาสตร์ จุฬาลงกรณ์มหาวิทยาลัย  
ปีการศึกษา 2564  
ลิขสิทธิ์ของจุฬาลงกรณ์มหาวิทยาลัย



ราพี แอล อาซ :

เทคนิคการสำรองโทนอนอย่างง่ายสำหรับการลดค่าอัตราส่วนระหว่างค่ายอดและค่าเฉลี่ยกำลังงานของสัญญาณการมัลติเพล็กซ์แบบแบ่งความถี่ตั้งฉาก. ( Simplified Tone Reservation-Based Techniques for Peak-to-Average Power Ratio Reduction of Orthogonal Frequency Division Multiplexing Signals ) อ.ที่ปรึกษาหลัก : ลัญจกร วุฒิสถิตกุลกิจ

การมัลติเพล็กซ์แบบแบ่งความถี่ตั้งฉากหรือโอเอฟดีเอ็มเป็นหนึ่งในเทคนิคการมอดูเลตที่จำเป็นสำหรับเครือข่ายการสื่อสารไร้สายสมัยใหม่ เนื่องจากมีประสิทธิภาพการใช้งานสเปกตรัมสูงและทนต่อช่องสัญญาณแบบเลือกความถี่ได้ อย่างไรก็ตามเป็นที่ทราบกันดีว่าสัญญาณโอเอฟดีเอ็มจะได้รับผลกระทบจากอัตราส่วนกำลังสูงสุดต่อค่าเฉลี่ยหรือพีเอพียอร์ขนาดใหญ่โดยสัญญาณโอเอฟดีเอ็มที่มีค่าพีเอพียอร์สูงจะถูกคลิป์โดยภาคขยายกำลังอย่างหลีกเลี่ยงไม่ได้ทำให้เกิดการบิดเบี้ยวของสัญญาณและการแพร่กระจายคลื่นนอกย่านความถี่ ส่งผลให้ประสิทธิภาพของอัตราความผิดพลาดของสัญญาณวิทยุวิทยุขึ้นมั่งเน้นไปที่รูปแบบของเทคนิคการลดพีเอพียอร์ที่เรียกว่า เทคนิคการสำรองโทนอนหรือทีอาร์ซึ่งมีคุณสมบัติที่ดีสามประการได้แก่ การลดพีเอพียอร์ลงได้มาก ไม่ต้องการข่าวสารข้างเคียงเพิ่มเติมที่เครื่องรับ และไม่มีการบิดเบี้ยวของสัญญาณของภายในย่านความถี่ โดยการสำรองโทนอนแบบควบคุมการคลิป์หรือซีซีทีอาร์เป็นหนึ่งในเทคนิคทีอาร์แบบวนซ้ำซึ่งสามารถลดค่าพีเอพียอร์ได้มาก แต่ต้องใช้เวลาในการคำนวณที่มีราคาแพง ดังนั้นวิทยุวิทยุขึ้นมั่งหวังที่จะนำเสนอเทคนิคที่มีพื้นฐานทีอาร์แบบใหม่ที่สามารถลดความต้องการด้านเวลาในการคำนวณในขณะที่ยังคงประสิทธิภาพการลดพีเอพียอร์ที่ใกล้เคียงที่สุดกับซีซีทีอาร์ โดยเทคนิคที่เสนอนี้ใช้การหาค่าเหมาะที่สุดแบบพาร์ติเคิลสวอรัมหรือพีเอสไอเพื่อกำหนดชุดสัญญาณการขดลวดที่เหมาะสม 8 รูปแบบที่กำหนดไว้ล่วงหน้าสำหรับเทคนิคทีอาร์ซึ่งช่วยเพิ่มอัตราขยายพีเอพียอร์อย่างมีนัยสำคัญและส่งผลให้สูญเสียสมรรถนะเพียง 0.5 dB เมื่อเทียบกับอัตราขยายพีเอพียอร์ของเทคนิคซีซีทีอาร์แบบดั้งเดิม โดยทั่วไปมีตัวจำแนกหลายแบบที่แตกต่างกันสำหรับการเลือกสัญญาณหักล้างที่เหมาะสมและใช้ในการจำแนกสัญญาณที่มีค่าพีเอพียอร์สูงและต่ำได้ ในที่นี้ได้เลือกใช้โครงข่ายประสาทเทียมหรือเอเอ็นเอ็นสำหรับภารกิจทั้งสอง ชั้นแรกคลาสโบนารีเอเอ็นเอ็นถูกใช้เพื่อจำแนกสัญญาณอินพุตว่ามีค่าพีเอพียอร์ต่ำและสูง จากนั้นใช้เอเอ็นเอ็นแบบหลายคลาสเพื่อเลือกสัญญาณหักล้างสำหรับอินพุตพีเอพียอร์สูง ด้วยเหตุนี้โมเดลเอเอ็นเอ็นนี้จึงช่วยลดเวลาในการคำนวณของเทคนิคการลดพีเอพียอร์ของทีอาร์ร่วมกับพีเอสไอที่เสนอต่อไป ในขณะที่ยังคงประสิทธิภาพการลดพีเอพียอร์ไว้เหมือนเดิม ผลลัพธ์เชิงตัวเลขแสดงให้เห็นว่าพีเอสไอที่มีทีอาร์เป็นพื้นฐานที่เสนอพร้อมตัวแยกประเภทเอเอ็นเอ็นแบบโบนารีและหลายคลาสสามารถบรรลุความแม่นยำโดยเฉลี่ยที่ 98% และ 95% ด้วยโมดูลตัวแยกประเภทเอเอ็นเอ็นแบบโบนารีและหลายคลาสตามลำดับ ในขณะที่เวลาในการคำนวณลดลงอย่างมาก 98% สำหรับคลื่นพาห่ของข้อมูลจำนวน 60 ความถี่

สาขาวิชา           วิศวกรรมไฟฟ้า  
ปีการศึกษา        2564

ลายมือชื่อนิสิต .....

ลายมือชื่อ อ.ที่ปรึกษาหลัก .....

# # 6272074721 : MAJOR ELECTRICAL ENGINEERING

**KEYWORD:** Peak to Average Power Ratio (PAPR), Orthogonal Frequency Division Multiplexing (OFDM), Particle Swarm Optimization (PSO), Tone Reservation (TR), Clipping Control Tone Reservation (CC-TR), Artificial Neural Network (ANN)

Rafee Al Ahsan : Simplified Tone Reservation-Based Techniques for Peak-to-Average Power Ratio Reduction of Orthogonal Frequency Division Multiplexing Signals . Advisor: Assoc. Prof. LUNCHAKORN WUTTISITTIKULKIJ, Ph.D.

Orthogonal Frequency Division Multiplexing (OFDM) is one of the preferred modulation techniques for modern wireless communications networks, due to its high spectral efficiency and immunity to frequency selective channels. However, OFDM signals are known to suffer from a large peak-to-average power ratio (PAPR). OFDM signals with high PAPR values will inevitably be clipped by the power amplifiers (PA), causing signal distortion and out-of-band radiation, that would lead to the deterioration of bit error rate performance. This thesis focuses on a class of PAPR reduction techniques called tone reservation (TR) techniques, which possesses three desirable features, namely high PAPR reduction gain, no side information required at the receiver, and no in-band distortion. Clipping Control Tone Reservation (CC-TR) is an iterative TR-based technique that can achieve high PAPR reduction gain but at the cost of expensive computational time requirements. Therefore, this thesis aims to provide a novel TR-based technique that has reduced computational time requirements while maintaining a PAPR reduction performance that is the closest to the CC-TR. The proposed technique uses the Particle Swarm Optimization (PSO) to determine a predefined efficient set of 8 proper canceling signals for the TR technique, which significantly improves PAPR reduction gain and result in approximately 0.5 dB loss of PAPR reduction gain when compared to the conventional CC-TR. There are different generic classifiers available for selecting proper peak canceling tones and classifying high and low PAPR OFDM signal classes. We select the ANN for both tasks. First, the binary class ANN is applied to classify the input to low and high PAPR input. Then, the multiclass ANN is applied to select the canceling signal for the high PAPR input. As a result, this ANN model reduces the computational time of the proposed TR-PSO PAPR reduction technique further while maintaining the same PAPR reduction performance. Numerical results show that the proposed TR-based PSO with binary and multiclass ANN classifier can achieve the average accuracy of 98% and 95%, with its binary and multiclass ANN classifier modules respectively, while significantly declining the computational time by 98% for 60 data subcarriers.

Field of Study: Electrical Engineering  
Academic Year: 2021

Student's Signature .....  
Advisor's Signature .....

## ACKNOWLEDGEMENTS

This Thesis work has been supported by the ASEAN and NON-ASEAN Scholarship of Chulalongkorn University.

Rafee Al Ahsan



# TABLE OF CONTENTS

	<b>Page</b>
ABSTRACT (THAI) .....	iii
ABSTRACT (ENGLISH).....	iv
ACKNOWLEDGEMENTS.....	v
TABLE OF CONTENTS.....	vi
LIST OF TABLES .....	1
LIST OF FIGURES .....	2
Chapter 1: Introduction.....	4
1.1. Motivation and Problem Statement .....	4
1.2. Research Objectives.....	4
1.3. Research Scope .....	4
1.4. Contributions .....	5
1.5. Literature Review .....	5
Chapter 2: OFDM and PAPR .....	9
2.1. Orthogonal Frequency Division Multiplexing (OFDM) .....	9
2.2. Peak-to-Average Power Ratio (PAPR).....	11
2.2.1. What is PAPR and How it is Calculated .....	11
2.2.2. How High PAPR Arises and its Problems .....	14
Chapter 3: Related Work .....	16
3.1. Tone Reservation (TR) .....	16
3.2. Clipping Control Tone Reservation (CC-TR) .....	17
3.3. Tone Reservation with Sphere Encoding (TR-SE).....	21
3.4. Simplified Clipping and Filtering (SCF) .....	26
Chapter 4: Proposed Methodology .....	29
4.1. Multi-level Mappings of Peak Canceling Tones .....	29
4.2. Modified Peak Canceling Tones Mapping Using PSO with TR .....	35

Chapter 5: Experiment and Discussion.....	41
5.1. Evaluation of TR-PSO:.....	41
5.2. Evaluation of TR-PSO with classifiers:.....	43
5.3. Comparison of PAPR reduction techniques .....	46
Chapter 6: Conclusion.....	52
REFERENCES .....	53
VITA.....	57





## LIST OF TABLES

	Page
Table 1. Computational Time analysis of Conventional TR at $L = 1,2,3,4$ .....	17
Table 2. Computational Time analysis of CC-TR for different mappings at $L = 3,4$ .....	21
Table 3. Computational Time analysis of TR with Sphere Encoder (TR-SE) for different mappings at $L = 1,2,3$ at different $\tau$ .....	25
Table 4. Computational time requirements of TR for different signal constellations with 1000 OFDM samples and $N = 13$ .....	34
Table 5. Computational time requirements of TR with PSO at $L = 1,2,3$ , for 1000 samples, $N = 13$ .....	43
Table 6. Test accuracy of multiclass ANN for TR-PSO at $N = 60$ and $L = 1,2,3$ for 10000 samples.....	45
Table 7. Computational time requirements of TR with PSO at $L = 1,2,3$ for 10000 samples, $N = 60$ .....	46
Table 8. Computational time requirements of the PAPR reduction techniques at $N = 13$ and $L = 1,2,3$ for 1000 samples.....	50
Table 9. Computational time requirements of the PAPR reduction techniques at $N = 60$ and $L = 1,2,3$ for 1000 samples.....	51
Table 10. Computational time requirements of the PAPR reduction techniques at $N = 124$ and $L = 1,2,3$ for 50 samples .....	51

## LIST OF FIGURES

	Page
Figure 1. OFDM Modulation procedure at the Transmitter.....	9
Figure 2. OFDM Demodulation procedure at the Receiver.....	10
Figure 3. CCDF vs PAPR for 16, 32, 64, 128, 256, 512, and 1024 subcarriers at QAM 4, $W = 1$ .....	13
Figure 4. CCDF vs PAPR for 16, 32, 64, 128, 256, 512, and 1024 subcarriers at QAM 4, $W = 4$ .....	13
Figure 5. CCDF vs PAPR for 16, 64, and 256 subcarriers at QAM 4, 16 and 64 at $W = 1$ ....	14
Figure 6. CCDF vs PAPR for 16, 64, and 256 subcarriers at QAM 4, 16 and 64 at $W = 4$ ....	14
Figure 7. Relation of Power of Input against Output for PA .....	15
Figure 8. CCDF vs PAPR curves for TR at $L = 1,2,3,4$ for (a) $N = 13$ and (b) $N = 60$ .....	16
Figure 9. Peak canceling action of CC-TR in OFDM with Clipping Impulse signals.....	18
Figure 10. Working Procedure of CC-TR.....	19
Figure 11. CCDF against PAPR (dB) for OFDM with CC-TR with $L = 1,2,3,4,5,6$ and (a) $CR = 3.90$ dB and (b) $CR = 2.93$ dB .....	20
Figure 12. CCDF against PAPR (dB) for OFDM with CC-TR with different number of iterations, $I$ , (a) $N = 13$ and (b) $N = 60$ .....	20
Figure 13. CCDF vs PAPR curves for TR-SE at $L = 1,2,3$ for $N = 13$ with different values of $\tau$ .....	24
Figure 14. CCDF vs PAPR curves for TR-SE at $L = 1,2,3$ for $N = 60$ with different values of $\tau$ .....	25
Figure 15. ICF algorithm PAPR reduction procedure .....	27
Figure 16. PAPR vs CCDF curves for SCF at different CR for (a) $W = 1$ and (b) $W = 4$ .....	28
Figure 17. Three well-known signal constellations .....	30
Figure 18. CCDF vs PAPR curves for TR, M-PSK, at $N = 13$ , $L = 1, 2, 3$ .....	31
Figure 19. CCDF vs PAPR curves for TR, M-ASK, at $N = 13$ , $L = 1, 2, 3$ .....	32
Figure 20. CCDF vs PAPR curves for TR, M-QAM, at $N = 13$ , $L = 1, 2, 3$ .....	33

Figure 21. Distribution of canceling tones used for PAPR reduction.....	35
Figure 22. CCDF distribution of each canceling tone of QAM-16.....	36
Figure 23. Particle Swarm Optimization .....	37
Figure 24. Distribution of canceling tones using PSO with the symmetric and normalized concept.....	39
Figure 25. Fitness characteristics of PSO .....	39
Figure 26. CCDF curves for comparison of PSO with and original QAM-16 at $L = 1, 2, 3$ ..	40
Figure 27. Distribution of 8 canceling tones.....	41
Figure 28. PDF of OFDM signals with $N = 13$ subcarriers .....	42
Figure 29. CCDF curves for comparison of PSO with and original QAM-16 at $L = 1, 2, 3$ ..	42
Figure 30. PDF of OFDM signals with $N = 60$ data subcarriers and $D = 30$ dummy subcarriers .....	43
Figure 31. Model of binary class ANN and multiclass ANN with the TR-PSO.....	44
Figure 32. CCDF vs PAPR curves for TR-PSO with and without ANNs for $L = 1, 2, 3$ .....	45
Figure 33. CCDF vs PAPR curves for PAPR reduction techniques for $N = 13, 60, 124$ at $L = 1$ .....	47
Figure 34. CCDF vs PAPR curves for PAPR reduction techniques, for $N = 13, 60, 124$ at $L = 2$ .....	48
Figure 35. CCDF vs PAPR curves for PAPR reduction techniques, for $N = 13, 60, 124$ at $L = 3$ .....	49

## Chapter 1: Introduction

### 1.1. Motivation and Problem Statement

Peak-to-Average Power Ratio (PAPR) has been a fundamental problem in Orthogonal Frequency Division Multiplexing (OFDM). This problem arises due to the constructive summation of multi-carrier signals resulting in occasionally high peak values of OFDM signals. These peak signals cause non-linear amplification of the power amplifiers at the transmitter, leading to unwanted in-band distortion and increased bit error rates. To handle the PAPR problem, different solutions already exist. Among them, Tone Reservation (TR) PAPR reduction techniques attract considerable attention, due to their three advantageous features, namely 1) inherent potential to achieve high PAPR reduction gain, 2) no in-band distortion arisen thereby bit error rate performance remains unchanged, 3) no side information is required by the receiver thus no loss in spectral efficiency. Some well-known TR-based techniques such as Clipping Control Tone Reservation (CC-TR), Tone Reservation with Sphere Encoding (TR-SE), have been already proposed. These techniques produce near accurate peak-canceling signals customized for each individual input data, such that the PAPR of a transmitted OFDM signal is minimized. However, these classes of Tone Reservation PAPR reduction techniques are known to require large computational time making them difficult for practical use in real-time transmission of OFDM signals. Therefore, it is interesting and very challenging to find other alternative PAPR reduction techniques that can maintain good PAPR reduction gains of these techniques, while the computational time required is reduced.

### 1.2. Research Objectives

The objective of this thesis is to provide a modified TR-based PAPR reduction technique that can use efficient peak-canceling signals that helps it to achieve significant PAPR reduction gain. Moreover, this thesis also aims to adopt a combination of classifiers as a tool to reduce the computational time requirements of the proposed TR-based PAPR reduction technique while maintaining the same PAPR reduction gain.

### 1.3. Research Scope

The scope of this thesis is to find and specify an appropriate fixed set of efficient peak canceling signals by simulation for achieving a good PAPR reduction gain for any given OFDM signal by experimentation. Then a model of a combination of binary class and multiclass classifiers is targeted to be experimented on regarding whether classifiers such as ANN can reduce the computational time of the search process for finding the appropriate peak canceling signals for the proposed model. ANN is adopted as the classifier for both tasks. Moreover, the binary class ANN module will be experimented on regarding whether it can correctly classify any given OFDM input symbols as high/low PAPR OFDM signal classes based on a pre-defined PAPR threshold level. Furthermore, the multiclass ANN module will also be targeted to be experimented on, regarding whether it can appropriately choose the proper peak canceling signals with high test accuracy on high PAPR OFDM signal classes only. The OFDM signals that will be used in our experiments are randomly generated and so it is assumed that the variables of the OFDM signals are independently and identically distributed Gaussian random variables as per the theorem of central limit. As a result, the OFDM signals' amplitudes follow Rayleigh distribution which causes the PAPR problem in real OFDM systems and the

occurrence of this PAPR problem is also seen in our simulated OFDM systems as well. The size of the subcarriers that will be mainly focussed on is 13 and 60. The evaluation quantity that will be used for measuring the PAPR reduction gain is the CCDF of PAPR values obtained from random OFDM signals. For measuring the computational time, the execution time of the conventional techniques, and the proposed technique with and without ANN classifiers will be measured.

## 1.4. Contributions

The contribution of this thesis is as follows:

1. The first contribution is that we have found and used a predefined set of finite and efficient canceling tones for the transmitter of OFDM signals to choose from instead of adopting the commonly known techniques such as CC-TR where the canceling tone values are tailored for each input signal. With a careful selection of 8 predefined canceling signal candidates from the 16 canceling signals found through the particle swarm optimization, it is shown by simulation that reasonably good PAPR reduction gain can be accomplished with less than 0.5dB loss of PAPR reduction gain as compared to the highly sophisticated CC-TR counterpart.
2. The second contribution is that the generic classifiers can be applied as a tool for achieving significantly reduced computational time i) for differentiating between high and low PAPR OFDM signals using the binary classifier, ii) for selecting a good canceling tone candidate from a predefined set of canceling signals using the multiclass classifier. ANN is adopted as a classifier in this thesis. We were also able to combine the ANN models to work cumulatively. We first apply the binary classifier ANN model on OFDM signal inputs to distinguish them in terms of high and low PAPR OFDM signals. Then secondly a multiclass ANN classifier model is applied on only the high PAPR OFDM signal classes for choosing the appropriate peak canceling signals found from using the TR-PSO technique. Furthermore, we also notice that the CCDF vs PAPR curves for our proposed combinations of ANN classifiers with the TR-PSO technique are identical to that of the alternative TR-based full search approach, thus they have the same PAPR reduction performance by reducing computational time by 98% for 60 subcarriers. Numerical results also show that our proposed binary class and multiclass ANN modules can attain high test accuracies of above 95% when both of them are combined to work cumulatively and automatically.

## 1.5. Literature Review

The main purpose of this survey is to identify the most relevant available studies related to PAPR reduction methods in OFDM systems.

OFDM was first established in 1967 for modulating multiple data bits for transmitting multi-subcarriers [1]. OFDM has many advantages such as it is spectrally efficient and can tolerate multipath fading, etc. However, OFDM has one major drawback referred to as the high Peak-to-Average Power Ratio (PAPR) problem. So to tackle this high PAPR problem in OFDM several PAPR reduction techniques have already been proposed in the literature. These PAPR reduction techniques can be classified into three different categories namely, Signal Distortion Techniques, Multiple Signaling and Probabilistic Techniques, and Coding Techniques.

The Signal Distortion Techniques are known to induce in-band distortion to the OFDM signals while minimizing their high PAPR. This further results in an increase of the Bit Error Rate (BER) of the transmitted OFDM signals on the receiver side. Some of the popular Signal Distortion PAPR reduction techniques include Clipping and Filtering [2], Peak Windowing [3], Companding [4], and Peak Cancellation [5].

Multiple Signaling and Probabilistic Techniques have two different types. The first type generates multiple combinations of OFDM signals with the use of peak reduction tones and finally transmits the OFDM signal that has the minimum PAPR. The second type adjusts the OFDM signals such that it has low PAPR by adding different shifts of phase or constellation points. The advantage of this technique is that it does not cause any in-band distortion to the OFDM signals. However, this technique may lead to a rise in the computational time of processing the OFDM signals for PAPR reduction. As well as in the case of the second type the information about the transformations of the OFDM signals' phases or constellations is needed to be known to both the transmitter and the receiver via side information, which is not required for the first type of this technique. So the need for side information for operating the second variant of this technique will lead to some loss of spectral efficiency. Some popular Multiple Signaling and Probabilistic Techniques are as follows: Tone Reservation (TR) [6],[7], Tone Injection (TI) [8], Selective Mapping (SLM) [9], Partial Transmit Sequence (PTS) [10], Interleaved OFDM [11], Active Constellation Shaping [12], Constrained Constellation Shaping [13].

Normally, the coding techniques can detect and correct errors for the binary bits received at the receiver of a wireless network for reducing BER. This ability of the coding techniques allows them to be adjusted for use in PAPR reduction of the same OFDM signals. However, most of the coding techniques often require some side information to be transmitted along with data subcarriers for proper decoding of the received signal. So this results in declining of the spectrum efficiency of the transmitted OFDM signal as well as also often causes an increase of computation time for processing the OFDM signals for PAPR reduction. The advantage of the coding technique is that it does not add any in-band distortion to the transmitted OFDM signal, so the BER of the received OFDM signal does not deteriorate. Some of the popular Coding Techniques used for PAPR reduction are as follows: Linear Block Coding [14], Golay Sequences [15], and Turbo Coding [16].

So from the three different types of PAPR reduction techniques mentioned above the Tone Reservation (TR) technique, which is a subset of Multiple Signaling, and Probabilistic Techniques PAPR reduction technique is focused on in this thesis. Tone Reservation is a type of PAPR reduction that was first proposed in 1997 by Polley and Gatherer as Clipping Control Tone Reservation (CC-TR) [7] and in 1999 by Tellado as gradient-based TR with a finite set of canceling candidates [6]. The TR technique that Tellado proposed used only a finite set of 4 canceling tones from the classic QAM-4 constellations for PAPR reduction. As a result, Tellado's TR PAPR reduction technique had very low computational processing time, but it also had low PAPR reduction gain due to using just a finite set of candidates. On the other hand, Polley's CC-TR PAPR reduction technique can acquire any arbitrary magnitude of the canceling tones for a given OFDM signal depending on a pre-defined threshold level. This allowed the CC-TR to have a higher PAPR reduction gain than the QAM-4 based TR however the CC-TR has very high computational time in contrast to TR.

In 2004, Krongold, et al. introduced another form of TR that is based on using Linear Programming (LP) combined with active set constraints as shown in [17] which can be

abbreviated as TR-LP. Similar to CC-TR the TR with LP also tries to find an arbitrary peak canceling tone for a given OFDM signal by solving many linear equations determined by the total number of subcarriers in an OFDM signal for minimizing the peak power. The advantage of the TR with LP is that it converges faster than the CC-TR for obtaining an efficient magnitude of canceling tones thus can attain better PAPR performance. However, the TR with LP can only work with real OFDM signals, and its computational time increases exponentially with the increase of the number of subcarriers making it difficult for use in real-time OFDM signal transmission.

In 2008, Krongold, et al. again proposed TR with the use of Quadratically Constrained Quadratic Program (QCQP) [18] for obtaining the canceling tones for complex baseband OFDM signals with the help of the active set approach. However, unlike Krongold's previous implementation which used LP with TR for real OFDM signal, this time Krongold's technique does not guarantee that it will achieve highly efficient peak canceling tones due to the power constraint. Moreover, the high computational time problem for processing the OFDM signals for PAPR reduction still remains in the TR with QCQP.

In 2011, Li, et al. implemented the use of the Least Square Approximation (LSA) technique for use with TR [19]. With just 2 iterations the LSA-TR can achieve the same approximate PAPR reduction gain as the CC-TR with 15 iterations with a reduction in computational time. However, the LSA-TR could not approximate the PAPR reduction performance of the CC-TR for a higher number of iterations such as 200 iterations, etc. As a result, the LSA-TR still lacked the PAPR reduction performance in contrast to the CC-TR using larger iterations.

In 2016, Fillippo, et al. proposed the use of TR with a set of canceling tones obtained with the help of Sphere Encoding algorithm from a quantized limited space of a multi-dimensional lattice [20]. Their technique showed a moderately higher gain of approximately 0.5 dB in its PAPR reduction performance in contrast to Krongold, et al.'s TR with QCQP algorithm. However, the TR with Sphere encoding (TR-SE) is sensitive to the chosen search step size. Large step sizes will lower the computational time, but the achievable gain may not be near-optimal. The use of smaller step sizes helps to improve the PAPR reduction gain but can radically increase the computational time.

In 2019, Jin, et al. proposed the use of Feed Forward Neural Network (FFNN) combined with Self Organizing Map (SOM) clustering technique to be used in TR algorithms for reducing the computational time of the CC-TR's working algorithm [21]. Moreover, in 2021, Jin, et al. have also adopted the use of the Extreme Learning Machine (ELM) technique instead of ANN as before for reducing the computational time of the CC-TR algorithm as well [22]. It appears that only these two research work uses predefined canceling signal sets obtained by using SOM from the CC-TR algorithm.

From our above review, we can group the work on TR into 5 categories: (1) an iterative search process for better PAPR reduction, [7], (2) an exhaustive search process from a set of canceling signals for PAPR reduction, [6],[20], (3) a quadratically or linearly solved programming process for finding canceling signals with high computational time for PAPR reduction [17],[18], and (4) a heuristic search approach for processing of fast PAPR processing with low PAPR reduction gain [19], (5) a PAPR reduction process using machine learning techniques [21], [22]. The iterative process has the best PAPR reduction at the cost of high computing time, so the researches on this topic are mostly based on designing the methods with

fast convergent rate using machine learning-based PAPR reduction techniques [21], [22]. So the above literature survey suggests that both PAPR reduction and computational time reduction are essential factors for efficient real-time transmissions of OFDM signals.

Moreover, based on the above literature survey, the TR technique has been chosen as the prime PAPR reduction technique in this thesis. This is because the TR does not add any in-band distortion to the transmitted OFDM signal like the Signal Distortion Techniques, so it causes no deterioration of BER of the received OFDM signals. Moreover, the TR technique does not require any side information to be transmitted, as a result it does not reduce the spectral efficiency, unlike the coding techniques. In addition, the TR technique also has a good potential to achieve high PAPR reduction gain as well. As we have seen that the different variants of TR mentioned above either suffer from a high PAPR reduction problem or high computational time problem or both. This thesis plans to tackle such problems in an efficient way that may help to reduce one or both of the problems based on certain aspects which will be discussed later in the next chapters.





## Chapter 2: OFDM and PAPR

### 2.1. Orthogonal Frequency Division Multiplexing (OFDM)

Orthogonal Frequency Division Multiplexing (OFDM) is a kind of digital modulation technique that is the adopted waveform of the current 4G-LTE and future 5G wireless communications. OFDM is a kind of Frequency Division Multiplexing (FDM) technique where each subcarrier is orthogonal to each other. This enables the prevention of interferences between subcarriers during parallel transmissions in OFDM. The subcarriers of OFDM are modulated by Quadrature Phase Shift Keying (QPSK) or Quadrature Amplitude Modulation (QAM) levels of 4, 16, 64, or 256. [23].

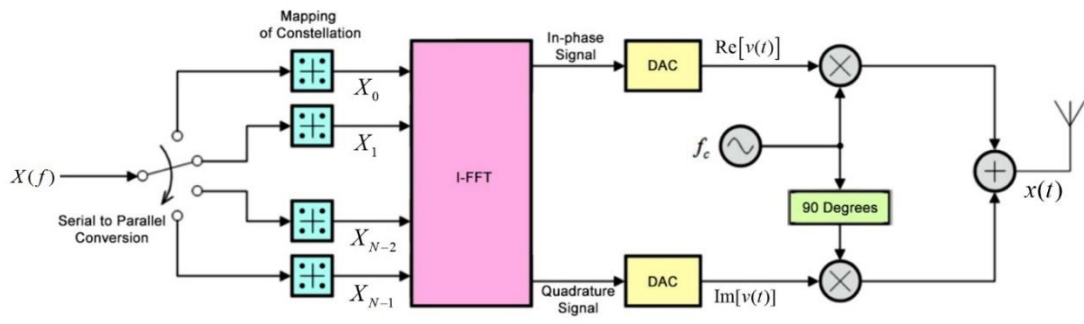


Figure 1. OFDM Modulation procedure at the Transmitter [6]

Figure 1 illustrates the modulation procedure of OFDM in the transmitter section. OFDM signals are generally formed by the total combination of  $N$  subcarriers, where each subcarrier is modulated by input data bits. The conversion of the combined OFDM bit patterns from serial to parallel depends on the QAM level assigned for each subcarrier. Different QAM level involves the mapping of different numbers of bits to a particular In-phase and Quadrature (IQ) symbol. QAM-4 maps 2 binary bits consisting of 0s and 1s in any order to one IQ symbol. Similarly, QAM-16, 64, and 256 maps 4, 6, and 8 binary bits sequences respectively to one symbol. After the constellation mapping process has been completed for each subcarrier, the OFDM I-Q symbols are obtained which can be written as follows:  $X(f) = \{X_k, k = 0, 1, \dots, N-1\}$  where  $X_k$  defines the I-Q symbols of the  $k$ -th I-Q OFDM subcarrier. After that, the Inverse Fast Fourier Transform (I-FFT) is applied to the complex I-Q symbols, to convert them from the complex frequency domain to complex time domains OFDM signals. These complex time-domain signals can be represented by eq. (2.1) [23]:

$$v(t) = \frac{1}{\sqrt{N}} \sum_{k=0}^{N-1} X_k e^{j2\pi k \Delta f t}, \quad 0 \leq t \leq T \quad (2.1)$$

In eq. (2.1),  $T$  is the total time duration of a particular OFDM symbol,  $\Delta f$  defines the gap in frequency between each subcarrier,  $j$  represents  $\sqrt{-1}$ ,  $\Delta f = 1/T$  and  $e^{j2\pi k \Delta f t}$  represents the twiddle factor [23]. Afterward, the complex OFDM time-domain signals are separated into In-phase (real) and Quadrature (imaginary) time-domain signals and are passed through Digital-to-Analog (DAC) converters. The DAC produces the analog time-domain signals of the

divided OFDM I-Q signals, which are then modulated with a carrier signal of frequency  $f_c$ . This process is known as the up-conversion of the transmitted OFDM signals. Finally, after upconverting  $v(t)$  in eq. (2.1) with carrier signal frequency of  $f_c$ , the transmitted OFDM signal can be shown by eq. (2.2) [23],[24].

$$\begin{aligned}
 x(t) &= \text{Re} \left\{ v(t) e^{j2\pi f_c t} \right\} \\
 &= \text{Re} \left\{ \frac{1}{\sqrt{N}} \sum_{k=0}^{N-1} X_k e^{j2\pi f_c t} e^{j2\pi k \Delta f t} \right\} \\
 &= \text{Re} \left\{ \sum_{k=0}^{N-1} |X_k| \arg[X_k] e^{j2\pi (f_c + k \Delta f) t} \right\} \\
 &= \sum_{k=0}^{N-1} |X_k| \cos \left( 2\pi \left[ f_c + \frac{k}{T} \right] t + \arg[X_k] \right)
 \end{aligned} \tag{2.2}$$

The OFDM symbols are then transmitted through an Additive White Gaussian Noise (AWGN) channel, which adds random distortion and noises to the transmitted OFDM signal.

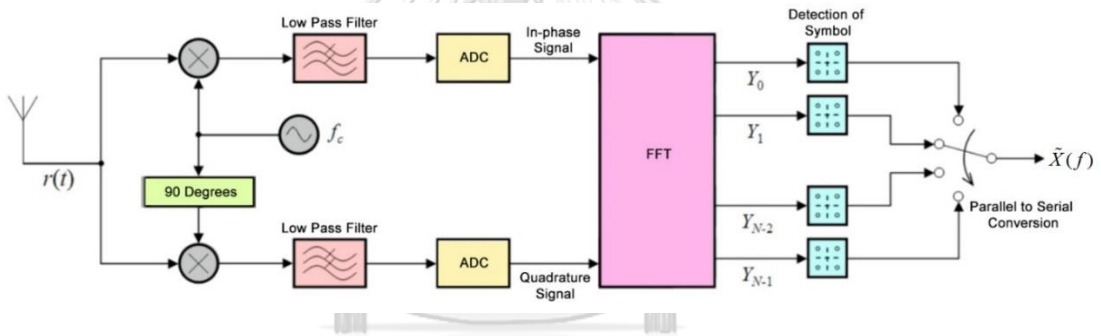


Figure 2. OFDM Demodulation procedure at the Receiver [6],[7]

Figure 2 shows the demodulation process of the noisy received signal,  $r(t)$ , for OFDM at the receiver. Here,  $r(t)$  is first down-converted to the baseband signal by multiplying 0 and 90 degrees phase-shifted versions of the carrier signal to it. Down converted  $r(t)$  produces two signals: one at the baseband frequency and the other at the double carrier frequency of  $2f_c$ . Therefore, the signals are passed through a low pass filter to eliminate the unwanted high-frequency component. After that OFDM signals are passed through an Analog-to-Digital Converter (ADC) which converts the time domain analog OFDM signal to digital OFDM signal. Then the digitized OFDM time-domain signals are Fast Fourier Transformed (FFT), which converts them back to the frequency domain. The received frequency domain OFDM signals can be written as follows:  $Y = \{Y_k, k = 0, 1, \dots, N-1\}$  where  $Y_k$  defines the received I-Q symbols of the  $k$ -th received I-Q OFDM subcarrier. Then each  $Y_k$  is detected based on its calculated Euclidean distance from a pre-defined constellation. This detection of I-Q symbols depends on the QAM levels assigned to the OFDM symbols during their transmission. Finally, the received bits are obtained from the detected QAM symbols, and then they are positioned

back from being parallel to serial format sequentially, to get the received binary bit sequence named as  $\tilde{X}(f) = \{\tilde{X}_k, k = 0, 1, \dots, N-1\}$  [23],[24].

The modulation for OFDM has many benefits for use in 5G wireless communications as follows [23],[24].

1. OFDM is largely spectrally efficient compared to other modulation schemes such as spread spectrum and sideband modulations,
2. OFDM does not require equalizations in the complex time domain for adjusting to poor channel conditions.
3. OFDM has high tolerance against co-channel interferences in the narrow band.
4. OFDM has large sturdiness in withstanding multipath fading and Inter-Symbol Interferences (ISI) among its subcarriers.
5. OFDM is very less sensitive to errors of time synchronization between transmitter and receiver.
6. OFDM does not require the usage of any filters in its transmitter and receivers compared to other modulation techniques like Universal Filtered Multi-Carrier (UFMC) and Filter Bank Multi-Carrier (FBMC) [23],[24].

However, OFDM also has some drawbacks for use in the 5G wireless communications as follows [23][24]:

1. OFDM is highly delicate towards Doppler shift, which occurs when both or either the transmitter or the receiver is not stationary. As a result, this changes the frequency of the transmitted and the received signal making it difficult to detect.
2. OFDM is very sensitive to errors of frequency synchronization between transmitter and receiver.
3. OFDM suffers from a high Peak-to-Average Power Ratio (PAPR), which reduces the overall power efficiency of communication systems relying on linear circuits of transmitters and receivers [25].
4. OFDM often loses some spectral efficiency due to the usage of cyclic prefixes or guard bands to combat poor channel conditions [23],[24],[25].

## 2.2. Peak-to-Average Power Ratio (PAPR)

### 2.2.1. What is PAPR and How it is Calculated

The Peak-to-Average Power Ratio (PAPR) of a given OFDM signal is normally calculated during its transmission in the time domain after the Inverse Fast Fourier Transform (I-FFT) has been applied to it. PAPR is calculated as the ratio of the maximum squared amplitude to the mean of the squared amplitudes of an OFDM signal as shown in eq. (2.3) [24],[26].

$$PAPR = \frac{\max\{|x(t)|^2\}}{E\{|x(t)|^2\}} \quad (2.3)$$

Following eq. (2.3), PAPR is often represented in decibels (dB) as illustrated in eq. (2.4) [24],[26]:

$$PAPR(dB) = 10 \log_{10} \frac{\max \{|x(t)|^2\}}{E\{|x(t)|^2\}} \quad (2.4)$$

The PAPR of the OFDM systems is often represented in terms of the Complementary Cumulative Distribution Function (CCDF). The CCDF helps to measure the performance of an OFDM signal regarding its probability to exceed a pre-defined threshold PAPR level. PAPR can be expressed in terms of CCDF because the complex OFDM signals are defined by variables that are random and are Gaussian distributed in the time domain. Because OFDM follows central limit theory as it has a large number of subcarriers,  $N$ . This random variable has a mean of 0 and a variance of 0.5. The amplitude of OFDM signals is Rayleigh distributed. Its power has the chi-squared distribution with 2 degrees of freedom. The CCDF of the OFDM signals in the time domain can be expressed by eq. (2.5) [24],[26]:

$$CCDF = \Pr(PAPR \geq PAPR_0) = (1 - (1 - e^{-PAPR_0}))^N \quad (2.5)$$

In eq. (2.5),  $PAPR_0$  is denoted as the threshold of a particular combination of OFDM symbols in a sample. However,  $PAPR_0$  varies from sample to sample for different combinations of OFDM complex symbols in the time domain. Eq. (2.5) gives the CCDF of the time domain OFDM signals which are sampled at the rate of Nyquist frequency. Sometimes oversampling is also required to obtain a better and accurate representation of the CCDF of the OFDM signals as shown in eq. (2.6) [24],[26]:

$$CCDF = \Pr(PAPR \geq PAPR_0) = (1 - (1 - e^{-PAPR_0}))^{WN} \quad (2.6)$$

In eq. (2.6),  $W$  is the oversampling factor and is taken as 4 [24],[26]. The PAPR of an OFDM signal can also be expressed in terms of Cubic Metric (CM), which provides a sense of scalability to the raw PAPR data obtained from an OFDM signal sample. This cubic metric for an OFDM signal in the time domain in decibel (dB) can be calculated as follows:

$$CM = \frac{RCM - RCM_{ref}}{K} \quad (2.7)$$

$$RCM = 20 \log_{10} \left\{ rms \left[ \left( \frac{|x(t)|}{rms[x(t)]} \right)^3 \right] \right\} \quad (2.8)$$

In eq. (2.7),  $RCM$  is denoted as the raw cubic meter, which is obtained by applying eq. (2.8) to a time-domain OFDM signal. In eq. (2.8)  $rms[\cdot]$  defines the operation of root mean square and in eq. (2.7),  $RCM_{ref}$  is the  $RCM$  of the reference signal and  $K$  is defined as the empirical factor [27].

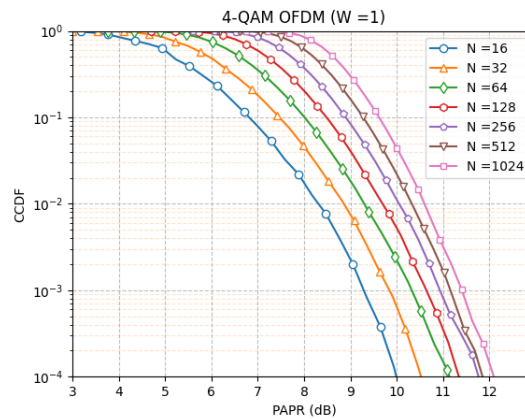


Figure 3. CCDF vs PAPR for 16, 32, 64, 128, 256, 512, and 1024 subcarriers at QAM 4,  $W =$

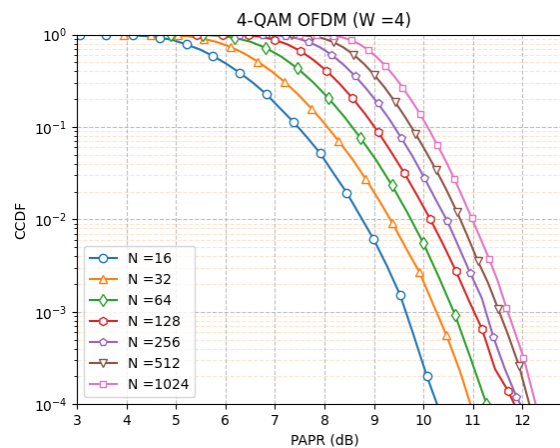


Figure 4. CCDF vs PAPR for 16, 32, 64, 128, 256, 512, and 1024 subcarriers at QAM 4,  $W =$

Figure 3 and Figure 4 show the graphs of CCDF against PAPR in dB unit for different numbers of subcarriers at QAM level of 4 and oversampling factor, ( $W$ ) of 1 and 4, respectively. Here the graph between PAPR and CCDF is approximated by the histogram of PAPR where the count is normalized by the total number of samples. 65536 OFDM samples were used, the entire PAPR range of 66536 samples are equally divided into a series of intervals. After that, the number of PAPR samples that fall within each series are counted cumulatively and normalized. These counts in the decreasing order represent the heights of the histogram in Figure 3 and Figure 4 which in turn depicts the simulated approximated CCDF curves [24],[26],[28].

A key property of the PAPR of OFDM signals has also been displayed in Figure 3 and Figure 4 which reveal that with the increase in the number of subcarriers from 16 to 1024, the curves of the CCDFs shift more to the right. This depicts that the probability of having higher PAPR also rises with an increase in the number of subcarriers at constant QAM levels and sample sizes [24],[26],[28]. Figure 3 and Figure 4 also show that the probability of high PAPR increases with an increase in oversampling factor,  $W$  [29].

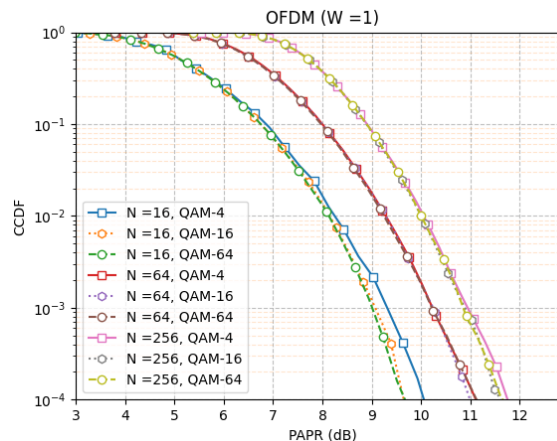


Figure 5. CCDF vs PAPR for 16, 64, and 256 subcarriers at QAM 4, 16 and 64 at  $W = 1$

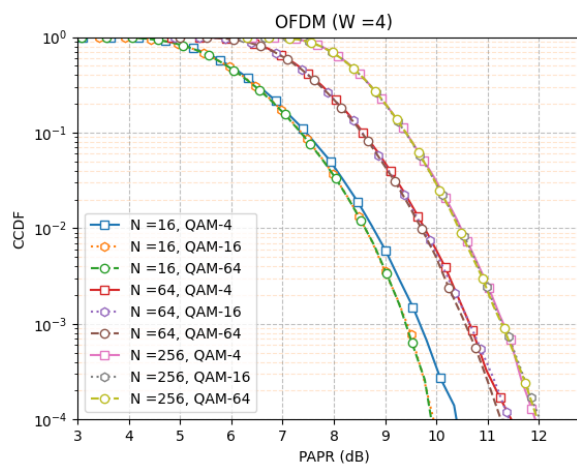


Figure 6. CCDF vs PAPR for 16, 64, and 256 subcarriers at QAM 4, 16 and 64 at  $W = 4$

Figure 5 and Figure 6 displays the CCDF against PAPR for 16, 64, and 256 subcarriers at different QAM levels at  $W = 1$  and  $W = 4$ . It is observed that increasing the number of bits has almost no impact on the PAPR of OFDM signals. This is because 4QAM, 16QAM, and 256QAM are assumed to have the same average power. We also know that 4QAM has only 4 signals, 16QAM has 16 signals and 256QAM has 256 signals. So for a large number of subcarriers, the sum of these random values will eventually converge to the same distribution, known as the Gaussian distribution with the same average power. Therefore, they will exhibit similar CCDF curves as shown above. Figure 5 and Figure 6 shows that  $N=16$ , 4QAM is shifting away from 16QAM and 64QAM. This is because, in the 4QAM case, we are summing only 16 subcarriers and the result has not converged properly to a Gaussian distribution yet [24],[26],[28],[29].

### 2.2.2. How High PAPR Arises and its Problems

In OFDM, high PAPR signals are produced when the analog time-domain signals generated from a certain number of combinations of I-Q symbols add up constructively together. This only occurs when the maximum peaks of several analog time-domain signals with the approximately same phase occur simultaneously during the modulation of the OFDM signals. As a result, this causes the final peak of those OFDM signals to project to a very high

magnitude compared to the average power of that OFDM signal, thus, creating high PAPR OFDM signals [26],[28],[30].

High PAPR is one of the most concerning problems of OFDM in wireless communication systems. Because high PAPR forces simple linear devices such as Power Amplifiers (PA) used with DAC and ADC to work in non-linear regions, during transmissions and receptions of OFDM signals, respectively. This introduces signal distortions in the converted analog and digitized signal during transmission and receptions of OFDM signals, respectively. Therefore, large PAPR results in the decline of the signal-to-quantization noise ratio (SQNR) for the PA [24],[26],[28],[30].

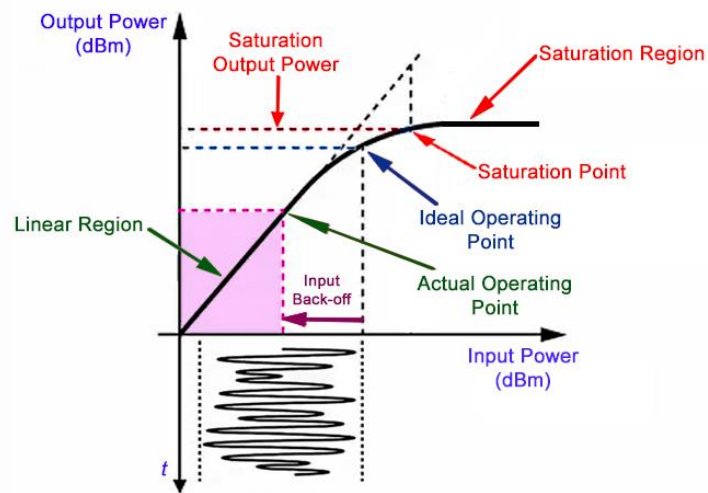


Figure 7. Relation of Power of Input against Output for PA [7],[12],[13]

Figure 7 demonstrates the power characteristics curve of input vs output for PA. To interpret the graph accurately, let us consider a numerical example. Suppose we have a PA, that is designed to operate at an average power of 15 Watts (W). This power in Watts is equivalent to 41.76-decibel milliwatts (dBm) which are calculated as follows:  $\text{Power(dBm)} = 10 \log(\text{Power (mW)})$ . If the PAPR of the OFDM signal for a certain sample is 11 dB, then the point of saturation of this PA will be at  $41.76 \text{ dBm} + 11 \text{ dB} = 52.76 \text{ dBm}$ . This power in dBm is equivalent to 188.84 W, which is computed as follows:  $\text{Power (mW)} = 10^{(\text{Power (dBm)}/10)}$ . Therefore, the PA is forced to amplify an OFDM signal with a large power of 52.76 dBm that is above its normal operating power of 41.76 dBm. A very large back-off power is required by the PA, which distorts the OFDM signal. As a result, the Bit Error Rate (BER) of the transmitted OFDM signal increases [24],[30].



## Chapter 3: Related Work

### 3.1. Tone Reservation (TR)

The tone Reservation (TR) technique can only choose a combination of reserved subcarriers that has the following values:  $\frac{1}{\sqrt{2}} + j\frac{1}{\sqrt{2}}$ ,  $\frac{1}{\sqrt{2}} - j\frac{1}{\sqrt{2}}$ ,  $-\frac{1}{\sqrt{2}} + j\frac{1}{\sqrt{2}}$  and  $-\frac{1}{\sqrt{2}} - j\frac{1}{\sqrt{2}}$  from QAM 4 modulation [6]. This is one of the desirable features of the TR technique since this allows the OFDM receiver to easily remove the peak canceling signals added by the TR without requiring any side information about the position of the reserved tones in the received OFDM signal. However, since the TR can only choose from a limited number of canceling signals it does not often obtain a very high substantial PAPR reduction gain [31].

The OFDM signal with TR can be formulated by using eq. (3.1) shown below:

$$\begin{aligned}\bar{x}[n] &= x[n] + c[n] \\ &= \text{I-FFT}(X_k + C_k) \\ &= \frac{1}{\sqrt{N}} \sum_{k=0}^{N-1} (X_k + C_k) e^{j2\pi kn/N}\end{aligned}\quad (3.1)$$

And the position of the data symbols and the canceling signals in a transmitted OFDM signal is shown in eq. (3.2) below:

$$X_k + C_k = \begin{cases} X_k, & k \in R^c \\ C_k, & k \in R \end{cases}\quad (3.2)$$

Where in eq. (3.2)  $R^c$  is a set of OFDM signals that carries data and  $R$  is a set of subcarriers that carries reserve tones for peak cancellation of OFDM signals [17],[31].

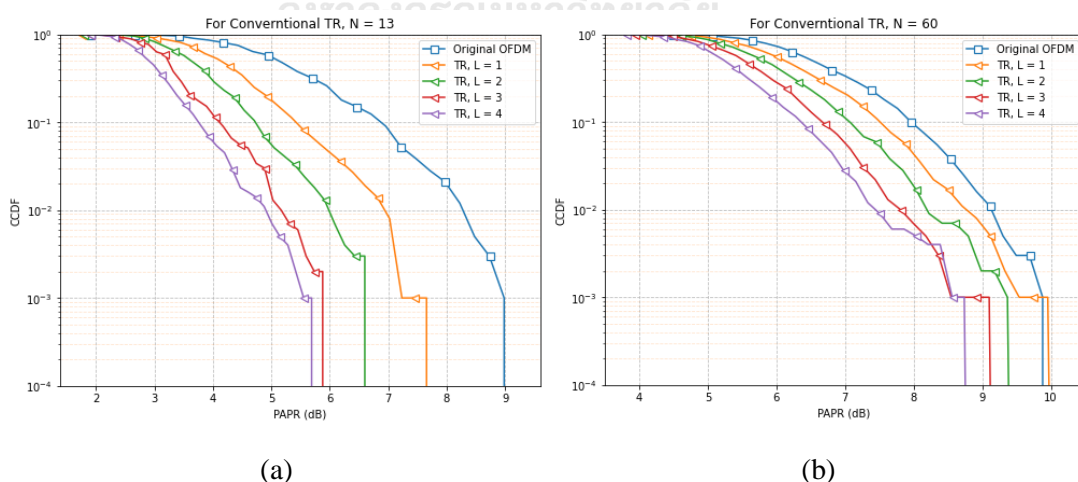


Figure 8. CCDF vs PAPR curves for TR at  $L = 1, 2, 3, 4$  for (a)  $N = 13$  and (b)  $N = 60$

Figure 8 shows the CCDF curve against PAPR for Tone Reservation at different numbers of canceling tones,  $L = 1, 2, 3, 4$  for  $N = 13$  and 60 subcarriers, respectively. Figure 8(a) shows



that as we increase the number of canceling tones from 1 to 4, the PAPR reduction gain of TR increases from 1.5, to 2.5, 3.1 and finally to 3.3 dB respectively for 13 subcarriers. Figure 8(b) shows for  $N = 60$  subcarriers, the gain in PAPR reduction is comparatively lower than that for  $N = 13$  subcarriers. But still, for  $N = 60$  subcarriers the gain also shows an increasing trend as well. Therefore, this overall suggests that the higher the number of canceling tones are the greater the strength the TR has in reducing the PAPR of a given OFDM signal. However, it is also seen that the TR technique also reaches a saturation point at some point when increasing the number of the canceling tone,  $L$ , does not give any substantial increase in PAPR reduction gain for the TR technique.

Table 1. Computational Time analysis of Conventional TR at  $L = 1,2,3,4$

Sample Size, ( $S$ )	Computational Time, ( $T$ ) (seconds)	Inputs	
		$N$	$L$
1000	2.4	13	1
	5.8		2
	19.2		3
	77.9		4
	8.9	60	1
	20.1		2
	67.2		3
	261.9		4

However, it should also be noticed that increasing  $L$  from 1 to 4 raises the computational time of the TR from 2.4 s to 77.9 s as shown in Table 1. And when we increase the number of subcarriers  $N$  from 13 to 60 subcarriers the computational time rises even higher to the range of 8.9 s to 261.9 s. So this is a drawback of using TR in the real-time transmissions of OFDM signals after processing them for minimizing the high PAPR OFDM signals.

### 3.2. Clipping Control Tone Reservation (CC-TR)

Normally, when an OFDM signal is generated for transmission, the number of FFT points,  $F$ , for the OFDM signals are usually greater than the number of data subcarriers,  $N$ . Therefore, this  $L = F - N$ , tones are the type of signals within the OFDM signals which represent  $0 + j0$  in the complex frequency domain as they carry no data. These extra tones,  $L$  are normally used to increase the frequency resolution of the OFDM signal for vivid analysis and viewing of frequency components that rapidly varies within close ranges [32].

Therefore, Clipping Control Tone Reservation (CC-TR) is a type of PAPR reduction technique that reserves these  $L$  tones to reduce the maximum peaks that tend to occur in an OFDM signal. These reserved  $L$  tones carry the time domain signal impulses, such that it is always opposite to the maximum peak amplitudes of the basic OFDM signal. The amplitude of these reserved  $L$  tones is determined by a pre-defined absolute clipping threshold amplitude,  $A$ . If the amplitude of an OFDM signal is greater than  $A$ , then the amplitude of the clipping signal

is equal to the maximum amplitude of the OFDM signal subtracted by  $A$  as shown in Figure 9. If the maximum amplitude of the OFDM signal is lower than,  $A$ , then the OFDM signal remains unchanged [7].

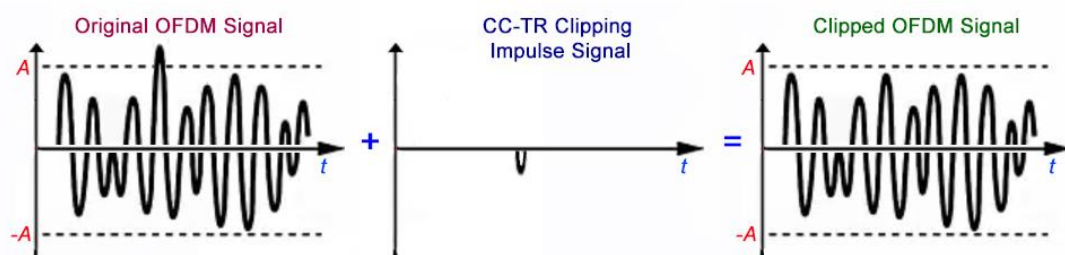


Figure 9. Peak canceling action of CC-TR in OFDM with Clipping Impulse signals

Mathematically the clipped signals of OFDM in the time domain can be expressed as follows [19]:

$$\tilde{v}_k = \begin{cases} v_k, & v_k < |A| \\ |A| e^{j\theta_k}, & v_k \geq |A| \end{cases} \quad (3.3)$$

In eq. (3.3),  $v_k$  is equal to  $|v_k| e^{j\theta_k}$  and  $\theta_k$  represents the phase of the  $k$ -th subcarrier [19]. Moreover, the peak reduction impulse signals of CC-TR in OFDM can also be written as shown in eq. (3.4) [19]:

$$f_k = \tilde{v}_k - v_k \quad (3.4)$$

These peak canceling signals of the CC-TR can be denoted as  $F_k$  in the frequency domain after performing FFT on it. Therefore, these complex  $F_k$  signals in the frequency domain should be positioned in such a manner that they do not overlap with the data-bearing subcarriers  $X_k$  to prevent distortion of data signals [33]. So the indexing of  $F_k$  signals is depicted by eq. (3.5) as follows [19]:

$$C_i = \begin{cases} F_i, & i \in R \\ 0, & i \notin R \end{cases} \quad (3.5)$$

In eq. (3.5),  $C_i$  represents the reserved version of the  $F_k$  peak canceling tones and it can be expressed as  $C = [C_0, C_1, \dots, C_{N-1}]^T$  and  $R$  denotes the index of the  $C$  reserved tones [31]. Moreover, the set of the indexes of the reserved tones,  $R$  in CC-TR can also be expressed as  $R = \{i_0, i_1, \dots, i_{L-1}\}$ , where  $L$  represents the total number of reserved tones [21]. Finally, the peak reduced OFDM transmitted signal can be written as  $(X + C)$  in the frequency domain, and its time-domain representation can be obtained by performing an I-FFT operation on it [19],[22].

The best feature of CC-TR is that it reduces the PAPR of a certain OFDM signal without degrading its BER [22]. The CC-TR follows a technique known as Fourier Projection Algorithm (FPA) to keep BER undistorted [7]. The FPA method is depicted in Figure 10 and is described as follows [7],[19]:

1. Set a value of the absolute threshold amplitude,  $A$ .
2. Perform I-FFT on the frequency domain OFDM signals,  $X(f)$  to get the time domain OFDM signals,  $v(t)$ , shown in eq. (2.1).
3. Find the peak amplitude of  $v(t)$ .
4. Compare the peak amplitude with the threshold level,  $A$ . Use eq. (3.3) to decide what happens to  $v(t)$ . If the maximum amplitude of the time domain OFDM signal is lower than  $A$ , keep  $v(t)$  unchanged and end the FPA process for this sample of OFDM signal. If the peak amplitude is greater than  $A$ , then set  $v(t) = A |e^{j\theta_k}|$ . This operation transforms the high peak time-domain OFDM signal,  $v(t)$ , into an OFDM signal,  $\tilde{v}(t)$  that has an absolute peak value equal to  $A$ . However, this transformation also adds BER to the OFDM data signals,  $\tilde{v}(t)$ . Therefore, to get rid of the distortion and reduce the BER, perform FFT again on the transformed  $\tilde{v}(t)$  and convert to the frequency domain  $\tilde{X}(f)$ . Then filtering is applied to get rid of the Out-of-Band (OoB) frequencies of the OFDM signals by zeroing them except the reserved tones,  $L$ . Then re-assign the frequency domain original data symbols back to  $\tilde{X}(f)$  using eq. (3.2) and eq. (3.5). Since the location of the reserved tones is already known from  $R$ , therefore, the reserved tones are kept unchanged, and the data symbols are updated to original values.
5. Perform I-FFT again on the  $\tilde{X}(f)$  to get  $\tilde{v}(t)$  and repeat step 4 until the maximum amplitude of the time domain OFDM signal is lower than  $A$ , and finally terminate the FPA process [7],[19],[22].

#### Clipping Control Tone Reservation (CC-TR)

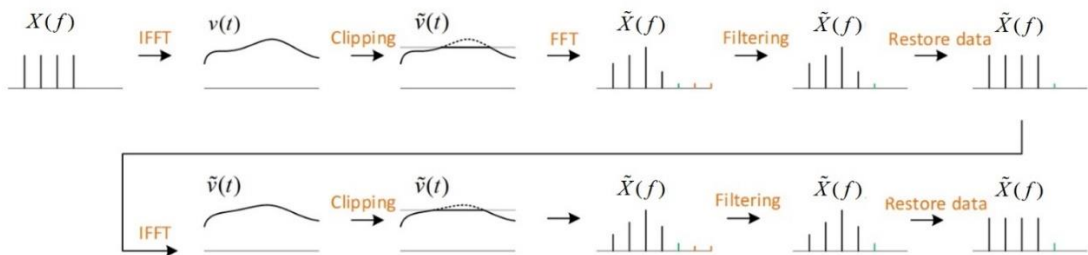


Figure 10. Working Procedure of CC-TR

The clipping ratio,  $CR$  of an OFDM signal for CC-TR is calculated using eq. (3.6) as described below [27]:

$$CR = \frac{A}{\sqrt{P_{av}}} \quad (3.6)$$

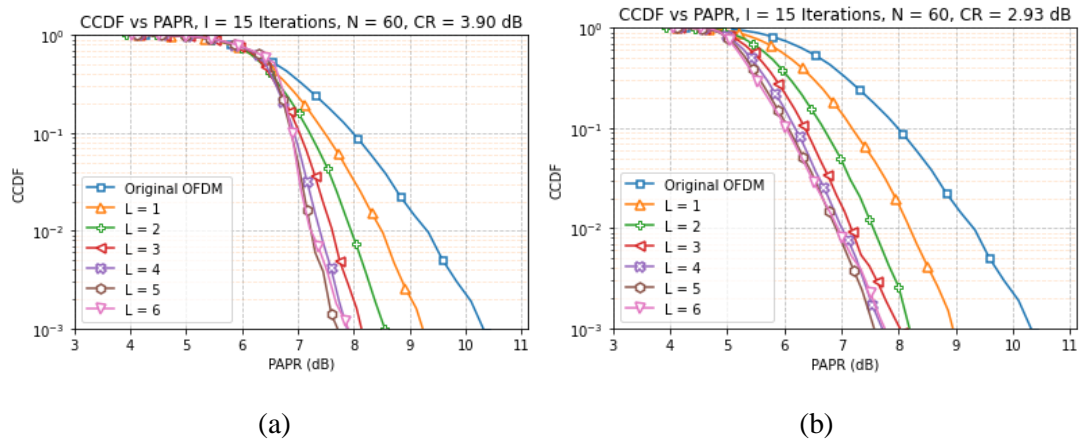


Figure 11. CCDF against PAPR (dB) for OFDM with CC-TR with  $L = 1, 2, 3, 4, 5, 6$  and (a)  $CR = 3.90$  dB and (b)  $CR = 2.93$  dB

Figure 11(a) and Figure 11(b) demonstrate the performance of CC-TR in OFDM in terms of PAPR reduction with the increase in the number of reserved tones,  $L$  from 1 to 6, and  $I = 15$  for Clipping Ratio ( $CR$ ) equal to 3.90 dB and 2.93 dB, respectively. Figure 11(a) shows that at  $CR = 3.90$  dB with the rise in the number of reserved tones,  $L$ , from 1 to 4, the PAPR reduction gain of the CC-TR algorithm significantly increases from 9.2 dB to 7.8 dB. However, when the reserved tones,  $L$ , are increased to higher values the PAPR reduction gains increase slightly to 7.7 dB. [22]. Figure 11(b) shows that at  $CR = 2.93$  dB with the rise in the number of reserved tones  $L$ , from 1 to 3, the PAPR reduction gain increases significantly. However, at high numbers of reserved tones, such as  $L = 4, 5, 6$ , the curves tend to saturate. This occurs because clipping level,  $A$ , is set to a high value in Figure 11(b) in contrast to Figure 11(a). As a result increasing the reserved tones,  $L$ , no longer increases the PAPR reduction ability of the CC-TR algorithm in Figure 11(b). Moreover, the above figures also show that the maximum peak canceling ability of CC-TR increases with the increase in the number of reserved tones,  $L$ . This occurs because a higher number of  $L$  reserved tones enables the CC-TR to produce more accurate peak canceling tones. As a result, the peak reduction in OFDM signals by the CC-TR becomes more prominent with the increase in  $L$  reserved tones [7].

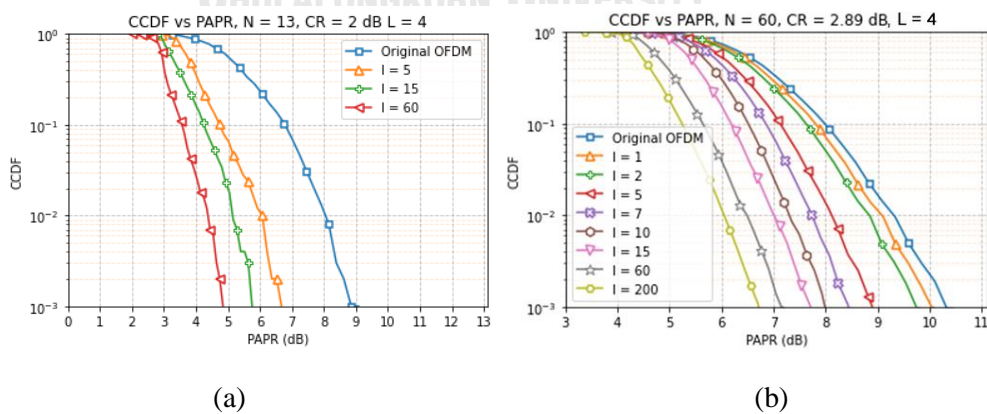


Figure 12. CCDF against PAPR (dB) for OFDM with CC-TR with different number of iterations,  $I$ , (a)  $N = 13$  and (b)  $N = 60$ .

Figure 12(a) and 3.5(b) show the PAPR curves for the CC-TR with  $N = 13$  and 60 subcarriers, with  $L = 4$  reserved tones and  $CR = 2$  dB and 2.89 dB, respectively, for different

numbers of iterations,  $I$ . From the curves, it can be seen that the PAPR reduction gain of the CC-TR increases with the increase in the number of iterations,  $I$ . This suggests that higher magnitudes of iteration,  $I$  result in greater PAPR reduction ability of the CC-TR. Because at higher iteration,  $I$  the CC-TR can produce more accurate peak canceling signals, the CC-TR attains higher PAPR reduction gains at the higher number of iterations,  $I$  [7],[22]. However, it must also be noted that the high number of iteration results in a vast increase of the computational time and is not appropriate for real-time transmissions and receptions. [7], [21],[22],[31]. Below are the results of the increase in computational time in the CC-TR due to an increase in  $N$  subcarriers,  $L$  reserved tones, and the number of iterations.

Table 2. Computational Time analysis of CC-TR for different mappings at  $L = 3,4$

Sample Size, ( $S$ )	Computational Time, ( $T$ ) (seconds)	Inputs		
		$N$	$I$	$L$
1000	3.2	13	5	3
	8.9		15	
	32.5		60	
10000	235.1	60	5	
	591.1		15	
	1650.3		60	
1000	4.1	13	5	4
	9.3		15	
	35.8		60	
10000	260.0	60	5	
	724.3		15	
	2428.5		60	

Table 2 shows that for  $N = 60$ ,  $L = 4$ ,  $S = 10000$  and  $I = 5$ , the computational time is 260.0 s. When we increase  $I$  from 5 to 60 for CC-TR, the computational time heavily increases by 9.4 times. The same behaviour of the increase in computational time is true for any  $N$ , and  $L$ . As a result, even though the PAPR reduction performance of the CC-TR increases with the increase in the number of iterations,  $I$ , its computational time increases exponentially, as a result it is highly difficult to use in real-time transmission of OFDM signals.

### 3.3. Tone Reservation with Sphere Encoding (TR-SE)

Tone Reservation with Sphere Encoding (TR-SE) is a type of PAPR reduction technique that uses an approach known as the tree-search for finding the canceling tones from a finite discrete space of a multi-dimensional lattice. During its search for suitable peak reduction signal candidates, the TR-SE algorithm has to follow a power constraint which states that the overall average energy per bit, ( $E_b$ ) of the canceling tones, must not exceed 1. The method of Sphere Encoding and Decoding is a well-known method for performing a full exhaustive tree-search in the space of candidates for obtaining efficient solutions [20]. Therefore, the optimization problem that the sphere encoder solves for minimizing PAPR is represented by eq. (3.7).

$$\begin{aligned}
& \min_{\lambda \in Z[j]^K} \|x(t) - \tau F_c \lambda\|_{\infty} \\
& \text{s.t. } \tau^2 \|\lambda\|_2^2 \leq \frac{K}{N-K} \|u\|_2^2
\end{aligned} \tag{3.7}$$

In eq. (3.7),  $Z[j]^K$  represents the  $K$ -dimensional lattice produced by the cartesian product of the Gaussian integer grid, where  $K$  is the number of reserved tones. Moreover,  $F_c$  is a  $K \times N$  matrix that performs I-FFT on  $\lambda$ , where  $N$  is the number of subcarriers, and  $x(t)$  is defined as the original time-domain OFDM signal.  $x(t)$  is also the center of the search region in the manner that it is the starting point in the search for the processed PAPR reduced OFDM signal. Moreover, in eq. (3.7)  $u$  is a  $N \times 1$  data signal matrix in the frequency domain with nulls or zeros in the place of reserved tones,  $\lambda$  is a discrete point of a lattice with  $K$  dimensions, and the scaling factor of the point,  $\lambda$  is controlled by the scaling factor  $\tau$ .  $\tau$  is arbitrarily set to any value in the range  $0 < \tau \leq 1$  in such a manner that the magnitudes of the complex canceling signals can be accurately found from the search space of the lattice which is real and quantized in nature. Smaller  $\tau$  provide a greater number of canceling tone candidates for PAPR reduction but it is also likely to increase the computational time of the TR-SE algorithm. Too small  $\tau$  may also cause diminishing capabilities of the TR-SE algorithm since decreasing  $\tau$  does not only increase the canceling tone candidates but also change the magnitudes of the canceling signal candidates. As a result, even though the canceling signal candidates are large in numbers at small  $\tau$ , but their changed magnitudes can also make them unsuitable for PAPR reduction performance. So  $\tau$  must be selected precisely to get the best performance of the TR-SE algorithm.

The TR with sphere encoding (TR-SE) can iteratively search for suitable peak canceling candidates for a maximum radius of  $R_1$  covering a multi-dimensional spherical region to reduce the peak value of an OFDM signal.  $R_1$  is defined by eq. (3.8) demonstrated below:

$$\|x(t) - \tau F_c \lambda\|_2^2 = \|u\|_2^2 + \tau^2 \|\lambda\|_2^2 \leq \frac{N}{N-K} \|u\|_2^2 \triangleq R_1^2 \tag{3.8}$$

So now before the TR with sphere encoding (TR-SE) can begin its search, it must know the maximum absolute peak of the OFDM signal that it will try to minimize. As a result, this maximum peak can be found using eq. (3.9) shown below:

$$\|x(t) - \tau F_c \lambda\|_{\infty} = \|x(t)\|_{\infty} \triangleq C_0 \tag{3.9}$$

So using the eq. (3.9) the radius,  $R_0$ , of the multi-dimensional sphere which consists of the maximum peak amplitudes can be computed using eq. (3.10) shown below:

$$\|u\|_2^2 = \tau^2 \|\lambda\|_2^2 \leq N C_0^2 \triangleq R_0^2 \tag{3.10}$$

Then after computing both the radius named as  $R_1$  and  $R_0$ , the TR with sphere encoder (TR-SE) restricts the position of its search region further and therefore the coordinate  $\lambda$  of its

movement for finding a suitable canceling tone follows the condition of in-equality shown below in eq. (3.11):

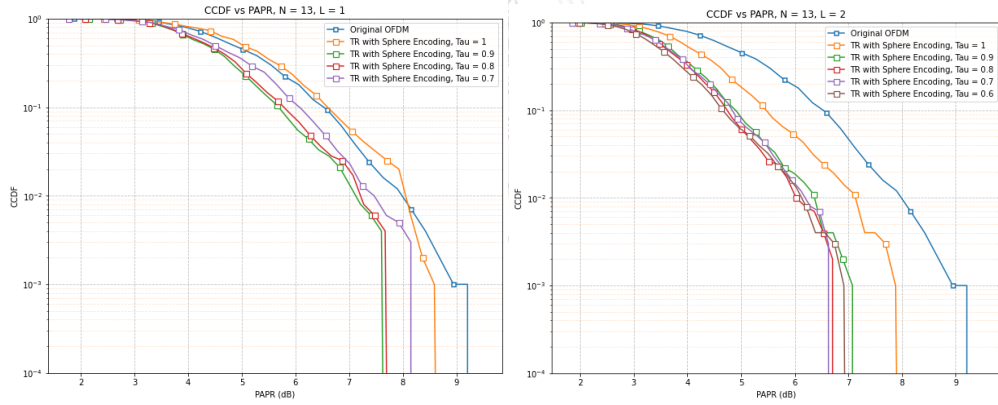
$$\|\lambda\|_2^2 \leq \frac{1}{\tau^2} \left( \min \{R_0^2, R_1^2\} - \|u\|_2^2 \right) \triangleq R_{\min}^2 \quad (3.11)$$

And the magnitude of  $\lambda$  eq. (3.11) are integers and vary in the boundary set by eq. (3.12) and eq. (3.13) depicted below:

$$\lambda_i = \left[ -A(\lambda_{i+1}^{K-1}), A(\lambda_{i+1}^{K-1}) \right], i = K-1, \dots, 0 \quad (3.12)$$

$$A(\lambda_{i+1}^{K-1}) = \left[ \sqrt{R_{\min}^2 - \sum_{j=i+1}^{K-1} |\lambda_j|^2} \right] \quad (3.13)$$

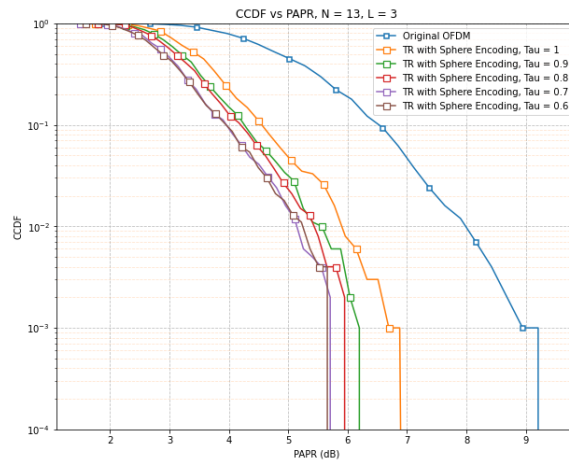
So based on eq. (3.12) and eq. (3.13), the TR with sphere encoder (TR-SE) searches a quantized and bounded space to find canceling tone candidates that lower the PAPR of an OFDM signal. It does this by visiting each of the different node points available to it and then it compares the PAPR value of the OFDM signal due to using the canceling tone in that node with the initial PAPR. If the node PAPR is lower than the current PAPR, it keeps that canceling tones but if it does not then it keeps on searching by moving to other nodes. However, the number of nodes that the TR with sphere encoder visits also increases exponentially with the increase in reserved tones, as a result, it also suffers from high computational time problems at a larger number of reserved tones [20].



(a)

(b)

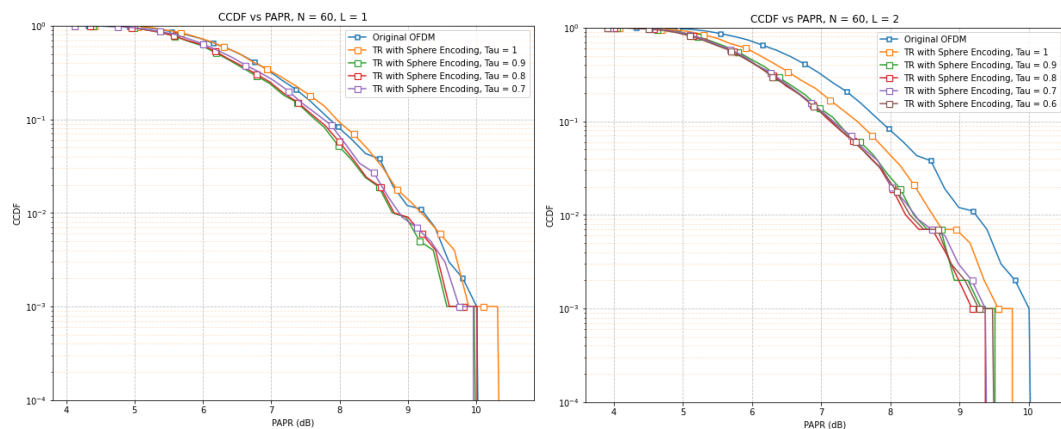




(c)

Figure 13. CCDF vs PAPR curves for TR-SE at  $L = 1, 2, 3$  for  $N = 13$  with different values of  $\tau$

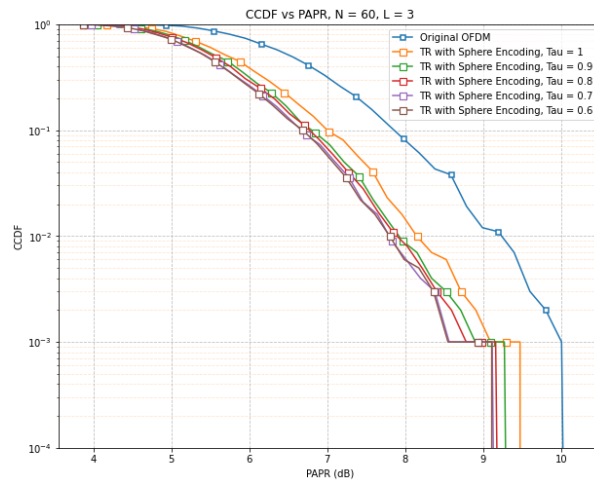
Figure 13(a), Figure 13(b), and Figure 13(c) demonstrate the CCDF versus PAPR curves for TR with sphere encoder (TR-SE) PAPR reduction technique with  $N = 13$  subcarriers by varying the number of reserved tones  $L$  to 1, 2, and 3, respectively for a total sample size of 1000 OFDM signals for different magnitudes of  $\tau$ . It can be seen vividly in the figures that different magnitudes of  $\tau$  are suitable for the different number of reserved tones  $L$ . In Figure 13(a), decreasing the magnitude of  $\tau$  from 1 to 0.9 shifts the CCDF curve of the TR-SE by approximately 1 dB to the left. This proves that the numbers and the magnitudes of canceling signal candidates obtained by the TR-SE from the quantized space lattice at  $\tau = 0.9$  are appropriate for increasing its PAPR reduction capabilities at  $L = 1$ . However, when  $\tau$  is further reduced to 0.8 and 0.7 the CCDF curves again start to shift to the right again. This suggests that even though the TR-SE now has access to higher numbers of canceling signal candidates, but their magnitudes are not appropriate for obtaining good PAPR reduction gain. As a result, the TR-SE suffers from diminishing PAPR reduction ability with the decreasing of scaling factor,  $\tau$ , below 0.9. In the case of  $L = 2$  canceling signals in Figure 13(b), and  $L = 3$  canceling signals in Figure 13(c), the CCDF curve of the TR-SE that shifts the most to the left are found at  $\tau = 0.8$  and  $0.7$ , respectively.



(a)

(b)





(c)

Figure 14. CCDF vs PAPR curves for TR-SE at  $L = 1, 2, 3$  for  $N = 60$  with different values of  $\tau$

Figure 14(a), Figure 14(b), and Figure 14(c) demonstrate the CCDF versus PAPR curves for TR with sphere encoder (TR-SE) PAPR reduction technique with  $N = 60$  subcarriers by varying the number of reserved tones  $L$  to 1, 2, and 3 respectively for a total sample size of 1000 OFDM signals for different magnitudes of  $\tau$ . For  $L = 1$  canceling signals in Figure 14(a),  $L = 2$  canceling signals in Figure 14(b), and  $L = 3$  canceling signals in Figure 14(c), the CCDF curve of the TR-SE that shifts the most to the left are found at  $\tau = 0.9, 0.8$  and  $0.7$ , respectively.

Table 3. Computational Time analysis of TR with Sphere Encoder (TR-SE) for different mappings at  $L = 1, 2, 3$  at different  $\tau$

Sample Size, ( $S$ )	Computational Time, ( $T$ ) (seconds)	Inputs		
		$N$	$L$	$\tau$
1000	4.2	13	1	0.9
	16.4		2	0.8
	51.3		3	0.7
	16.2	60	1	0.9
	67.8		2	0.8
	730.9		3	0.7

Table 3 shows that increasing the value of  $L$  from 1 to 3, with the reduction of  $\tau$  from 0.9 to 0.7 to get the best PAPR reduction performance of the TR-SE raises its computational time from 4.2 s to 51.3 s for  $N = 13$  subcarriers as shown above. And when we increase the number of subcarriers,  $N$  from 13 to 60 subcarriers the computational time raises even higher to the range of 16.2 s to 730.9 s. This increase in computational time occurs because the search region increases exponentially with the increase in  $L$  canceling signals and with the decrease in the scaling factor,  $\tau$ .

### 3.4. Simplified Clipping and Filtering (SCF)

Clipping and Filtering (CF) is a type of PAPR reduction technique that involves cutting of maximum peaks of OFDM signals in time domain above a certain threshold level,  $A$ , and then filtering is done on the clipped OFDM signal in the frequency domain by zeroing out the complex Out-of-Band (OoB) OFDM signal frequencies. The CF technique is one of the most popular PAPR reduction techniques for OFDM signals since they have very little computational time for reducing peaks of OFDM signals [34],[35],[36].

But it must also be noted that filtering an OFDM signal's OoB frequency spectrum often results in the reappearance of the high PAPR OFDM signals above the threshold level,  $A$ . So it is not often adequate to run the CF PAPR reduction technique for just one time as the desired low peak amplitude for OFDM signals is very less likely to be obtained with just  $I = 1$  iteration for CF PAPR reduction techniques. Therefore, a version of the CF known as the Iterative Clipping and Filtering (ICF) has been implemented in [37],[38] for repeating the clipping and filtering several times to diminish the reappearing high peaks prominently. Below are the steps for how the ICF is carried out accordingly:

1. First, the ratio of clip level ( $CR$ ) has to be set. Moreover, the total number of iterations,  $R$  must also be fixed before the first iteration can initiate. The  $CR$  for the ICF can be calculated using eq. (3.14) shown below:

$$CR = \frac{A}{\sqrt{P_{av}}} \quad (3.14)$$

In eq. (3.14),  $A$  represents the set threshold clip level and  $P_{av}$  represents the average power of the OFDM signal.

2. After that, the OFDM signal in the time domain,  $v(t)$ , is found by taking the I-FFT operation of frequency-domain OFDM signals,  $X(f)$ .
3. Then the time domain OFDM signals,  $v(t)$ , will be clipped using equation (3.3). So those OFDM signals are that are above  $A$  are clipped, and those below  $A$  remain unchanged.
4. Perform FFT operation on the clipped time-domain OFDM signals,  $\tilde{v}(t)$ . Then any OoB frequencies of the OFDM signal in the frequency domain are filtered out. Filtering operation re-initializes the OoB frequencies as  $0 + j0$  for the frequency domain OFDM signals,  $\tilde{X}(f)$ .
5. Repeat steps 2-4 for  $I$  iterations [2],[27].

### Iterative Clipping and Filtering (ICF)

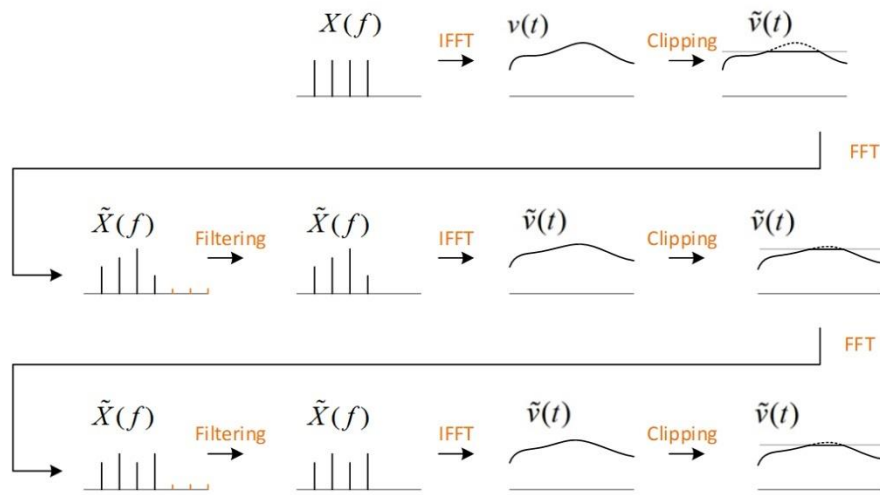


Figure 15. ICF algorithm PAPR reduction procedure

Figure 15 demonstrates the iterative procedure of PAPR reduction of the ICF as discussed above. However, since ICF is an iterative process, it also suffers from increased computational time similar to the CC-TR. Therefore, to reduce the computational time of the ICF, another PAPR reduction variant technique of the CF method has been discussed in [2],[27]. This PAPR reduction method is named as the Simplified Clipping and Filtering (SCF) technique. The SCF technique can be considered as a simplified version of the ICF technique discussed above. In the SCF technique, clipping is done in the conventional ICF technique in a scaled manner. The scaling of clipping is done in such a way that the SCF can achieve the same PAPR reduction of an OFDM signal with just 1 iteration, while the ICF require 3 iterations to obtain the same CCDF distribution of PAPR for a certain number of samples of OFDM signals[27],[2].

The SCF algorithm can be summarized as follows:

1. In the first step a time-domain version of an OFDM signal,  $\tilde{v}_k$ , that has been clipped using eq. (3.3) is obtained by doing I-FFT operation.
2. Then in the second step, the clipping noise of the time domain OFDM signal is computed using eq. (3.15) demonstrated below:

$$f_k = \tilde{v}_k - v_k \quad (3.15)$$

3. In the 3<sup>rd</sup> step, the frequency domain version of the clipping noise,  $F_k$ , is computed by performing an FFT operation on  $f_k$ .
4. Afterward, the filtering operation is carried out on the clipping noise,  $F_k$ , in the frequency domain, by zeroing out the OoB frequencies as displayed in eq. (3.16) below:

$$\tilde{F}_k = \begin{cases} F_k, & 0 \leq k \leq N/2 - 1, NJ - N/2 + 1 \leq k \leq NJ - 1 \\ 0, & N/2 \leq k \leq NJ - N/2 \end{cases} \quad (3.16)$$

5. Then an approximated clipped OFDM signal is obtained in the frequency domain by subtracting the original signal,  $X(f)$  by the filtered clipped noise,  $\tilde{F}_k$ , which is scaled by  $\bar{\beta}$  as shown in eq. (3.17):

$$\tilde{X}(f) = X(f) - \bar{\beta} \tilde{F}_k \quad (3.17)$$

In eq. (3.17),  $\bar{\beta}$  is represented by eq. (3.18) as shown below:

$$\bar{\beta} = \frac{1 - (1 - \bar{\alpha})^{3k/2}}{1 - (1 - \bar{\alpha})^{3/2}} \quad (3.18)$$

In eq. (3.18),  $\bar{\alpha}$  can be defined by eq. (3.19) as demonstrated below:

$$\bar{\alpha} = \frac{2\sqrt{2} / \sqrt{3\pi}}{\sigma / A} \quad (3.19)$$

In eq. (3.19),  $A$  is defined as the set clipping threshold level or amplitude and  $\sigma$  is known as the standard deviation of the OFDM signals that follows the complex gaussian distribution.

6. Finally, the time domain OFDM signal,  $\tilde{v}(t)$ , is obtained by performing I-FFT on the frequency domain OFDM signals,  $\tilde{X}(f)$ .

However, it must also be observed that the approximation by the SCF is only appropriate for 3 iterations of the ICF PAPR reduction technique. If higher values of iterations,  $I$ , are required then it fails to achieve this task. As well as both the SCF and ICF adds distortion to the OFDM signal which results in the rise of BER as shown in [2],[27].

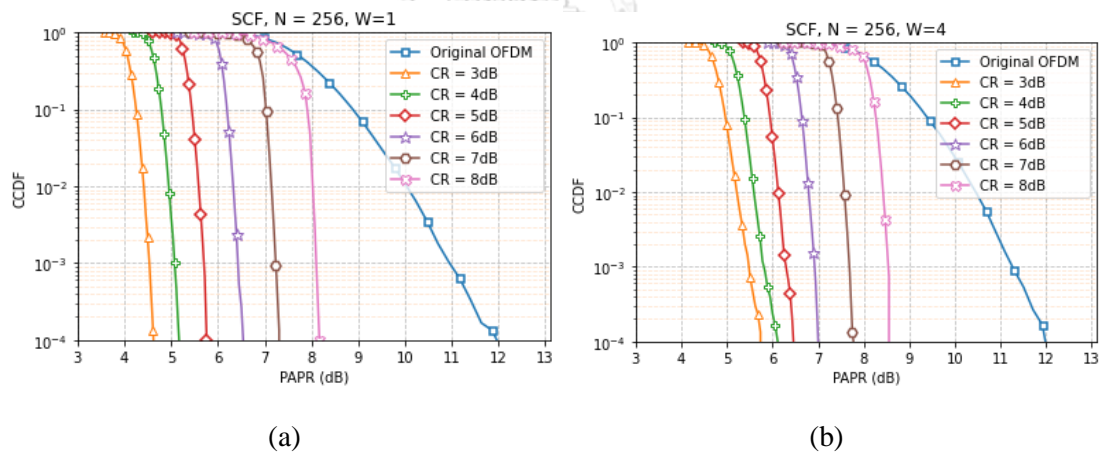


Figure 16. PAPR vs CCDF curves for SCF at different CR for (a)  $W = 1$  and (b)  $W = 4$

Figure 16(a) and Figure 16(b) show the CCDF curves for SCF at different magnitudes of Clipping Ratios (CR) at two different oversampling factors of  $W = 1, 4$ . As shown clearly in the figures that the increase in  $W$  at similar CRs increases the PAPR of a given OFDM signal. As well as it can also be seen that increasing the CR also increases the PAPR of a certain OFDM signal since the clipping threshold level,  $A$ , is set to a higher value. As a result, fewer OFDM signals are clipped at higher magnitudes of  $A$ , so PAPR increases [2],[27].

## Chapter 4: Proposed Methodology

In this chapter, we first give a review of the available fixed set of pre-defined canceling signals such as M-ary Phase Shift Keying (M-PSK), M-ary Amplitude Shift Keying (M-ASK), and M-ary Quadrature Amplitude Modulation (M-QAM) for use in Tone Reservation (TR) in section 4.1. And then we compare their performances in terms of PAPR reduction gain and computational time to find their pros and cons for use in real-time transmission of OFDM systems. Moreover, in section 4.2 we choose the peak canceling signals of the 16-QAM PAPR reduction technique and further enhance the peak canceling signals for gaining a higher PAPR reduction gain using the Particle Swarm Optimization (PSO) technique with the constraint that the overall average energy per signal,  $E_c$  of the canceling signals, is one.

### 4.1. Multi-level Mappings of Peak Canceling Tones

In the conventional TR, the canceling tone signals are chosen from the same mapping signals as that of data subcarriers primarily to simplify the practical implementation. In this study, for example, we have adopted the 4-QAM signal mapping for data symbols. Hence the canceling tone signals used by the conventional TR will also be 4-QAM. This means that only 4 choices of signals, namely  $\frac{1}{\sqrt{2}} + j\frac{1}{\sqrt{2}}$ ,  $\frac{1}{\sqrt{2}} - j\frac{1}{\sqrt{2}}$ ,  $-\frac{1}{\sqrt{2}} + j\frac{1}{\sqrt{2}}$  and  $-\frac{1}{\sqrt{2}} - j\frac{1}{\sqrt{2}}$  are made available for the purpose of PAPR reduction. Consequently, the achievable PAPR reduction gain is rather limited. A common means to resolve this problem is by introducing more canceling tones, *i.e.*,  $L > 1$ . Since a higher number of canceling tones mean greater combinations of peak canceling signals to choose from. Let  $B$  be the total number of bits assigned to each canceling tone, the total number of distinct canceling signals is  $2^{L \cdot B}$ . It is important to emphasize that the increase in the number of canceling tones will cause a reduction of the spectral efficiency of the OFDM system.

In order to provide more combinations of canceling signals, we propose in this thesis to utilize the higher orders of OFDM symbol mappings, namely M-ary Phase Shift Keying (M-PSK), M-ary Amplitude Shift Keying (M-ASK), and M-ary Quadrature Amplitude Modulation (M-QAM), where their constellations are displayed in Figure 17(a)-(c), respectively. M-PSK and M-ASK can offer much more variety in phases and amplitudes of the peak canceling tones respectively whereas M-QAM provides the combinations of both amplitudes and phases. The following experiments will comprehensively identify which of the extended mappings below will better improve the PAPR reduction gains.

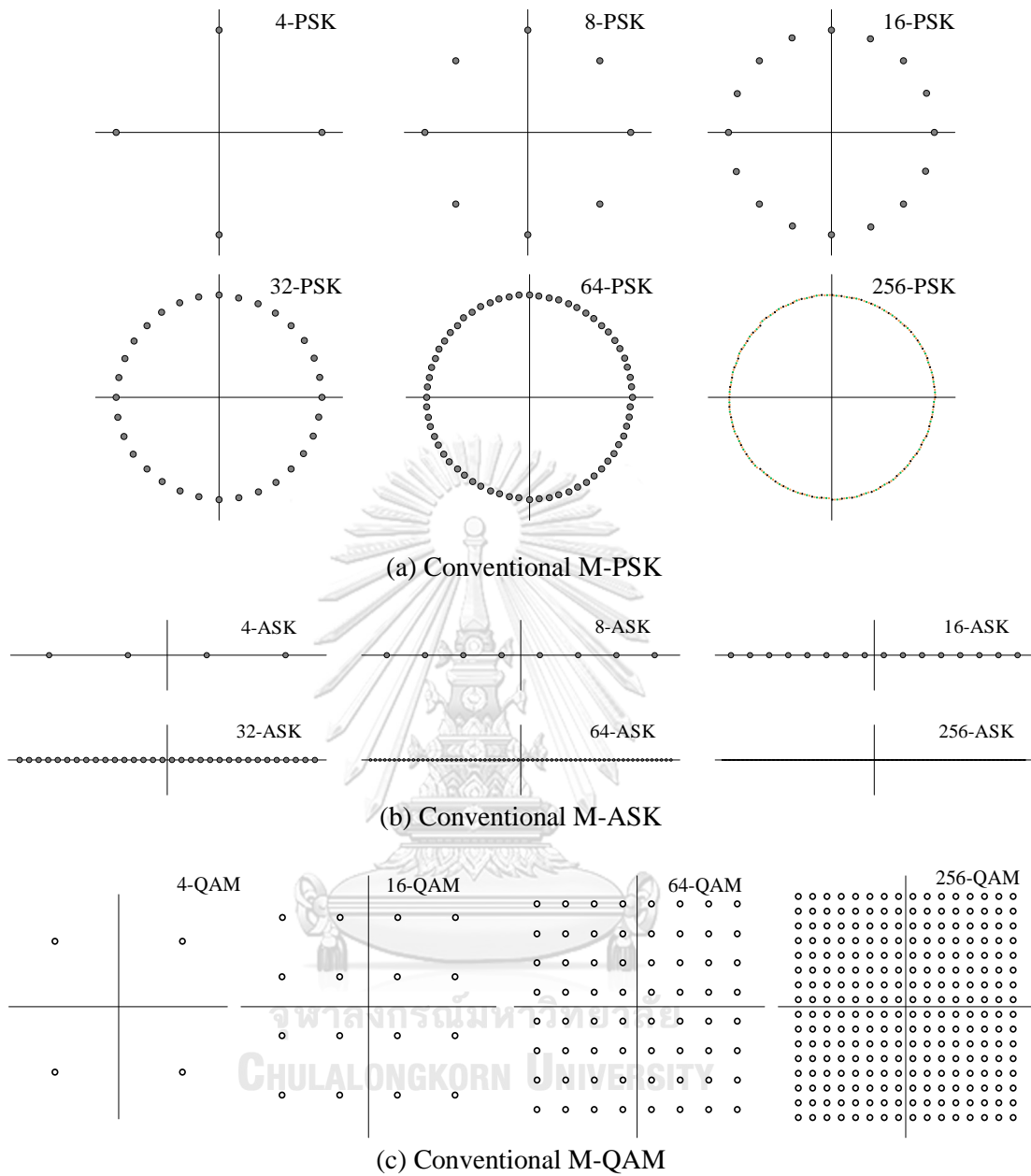


Figure 17. Three well-known signal constellations

**M-PSK canceling tones:**

The M-ary Phase Shift Keying (M-PSK) signal constellation is defined as shown by eq.(4.1):

$$s_k = \sqrt{E_c} \exp\left(\frac{j2\pi k}{M}\right), \quad k = 0, 1, 2, \dots, M-1 \quad (4.1)$$

where  $E_c$  is the average energy per canceling signal. Each M-PSK signal used for peak reduction is normalized to have the same unit energy, i.e.,  $E_c = 1$ . Figure 17(a) depicts M-PSK

signal constellations for  $M = 4, 8, 16, 32, 64,$  and  $256$ . In order to evaluate the PAPR performance of the OFDM systems using the M-PSK canceling signals, computer simulations have been conducted to determine the complementary cumulative distribution function (CCDF) of PAPR with a small number of data subcarriers  $N = 13$  and the varied number of canceling tones  $L = 1, 2, 3$ . Numerical results for the CCDF are depicted in Figure 18. At  $\text{CCDF} = 10^{-3}$ , the PAPR reduction gains of 1 dB, 2 dB, and 3 dB can be obtained for 4-PSK with  $L = 1, 2, 3$  respectively in contrast to original OFDM. This means that an increase in the number of canceling tones from 1 to 3 can enhance the PAPR reduction gains. However, when the number of canceling signal candidates is increased from 4-PSK to higher-order signal constellations such as 8-PSK, additional PAPR reduction gains are observed, not substantial though. Further increases in the number of canceling signal candidates to 16-PSK, 32-PSK, 64-PSK, and 256-PSK give almost no improvement.

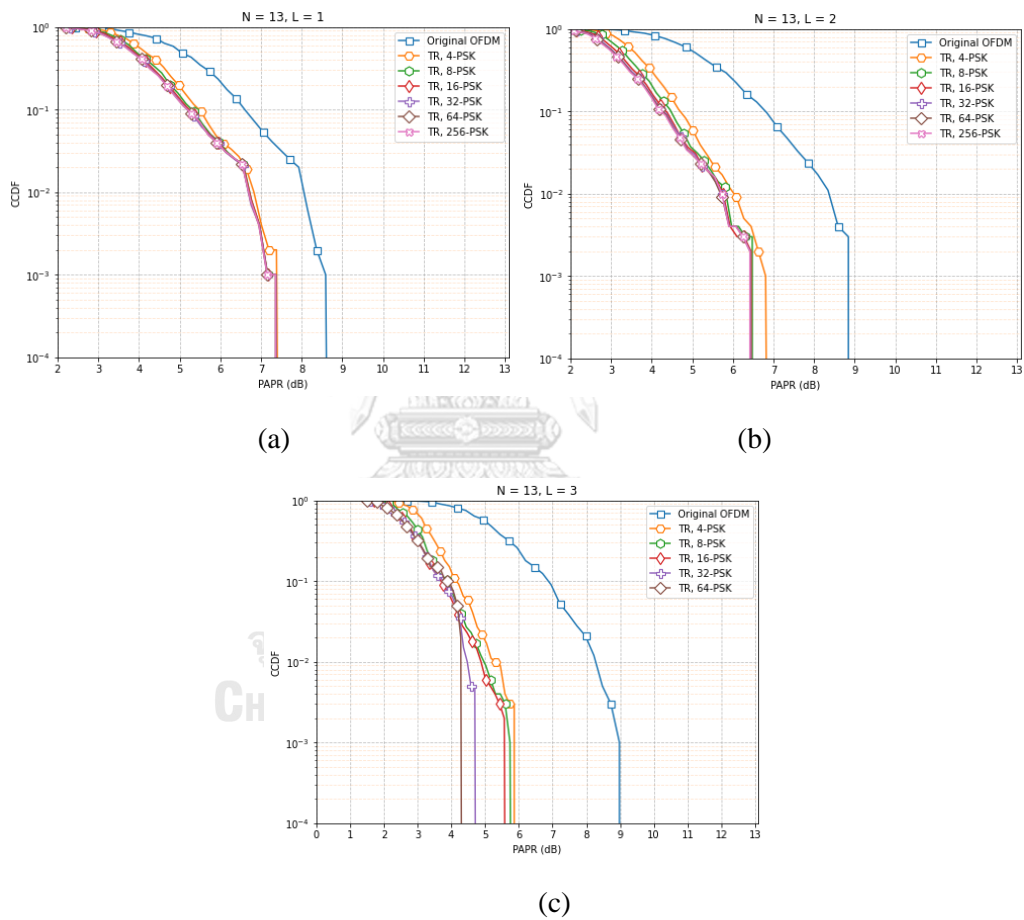


Figure 18. CCDF vs PAPR curves for TR, M-PSK, at  $N = 13, L = 1, 2, 3$

#### M-ASK canceling tones:

The M-ary Amplitude Shift Keying (M-ASK) signal constellation is defined as shown by eq.(4.2):

$$s_k = (2 \times k - M + 1) \times \sqrt{\left( \frac{3}{M^2 - 1} \right) \times E_c} \quad k = 0, 1, 2, \dots, M - 1 \quad (4.2)$$



where  $E_c$  is the average energy per canceling signal. M-ASK symbols used for peak reduction have varied amplitudes with the same phase of zero. The average energy per symbol is normalized to one,  $E_c = 1$ . Figure 17(b) represents M-ASK signal constellations for  $M = 4, 8, 16, 32, 64,$  and  $256$  used in our experiments. Figure 19 shows the CCDF against PAPR curves for different M-ASK signals of canceling tones at  $L = 1, 2, 3$  respectively. It is clear that PAPR reduction gains can be improved by increasing the number of canceling tones. At  $\text{CCDF}=10^{-3}$ , the 4-ASK approximately achieves the gains of 1 dB, 2.5 dB, 3 dB in contrast to the original OFDM for  $L = 1, 2, 3$  respectively. However, when the number of signal candidates is increased from  $M = 4$  to  $M = 8, 16, 32, 64,$  and  $256$ , the PAPR reduction gains are marginally increased.

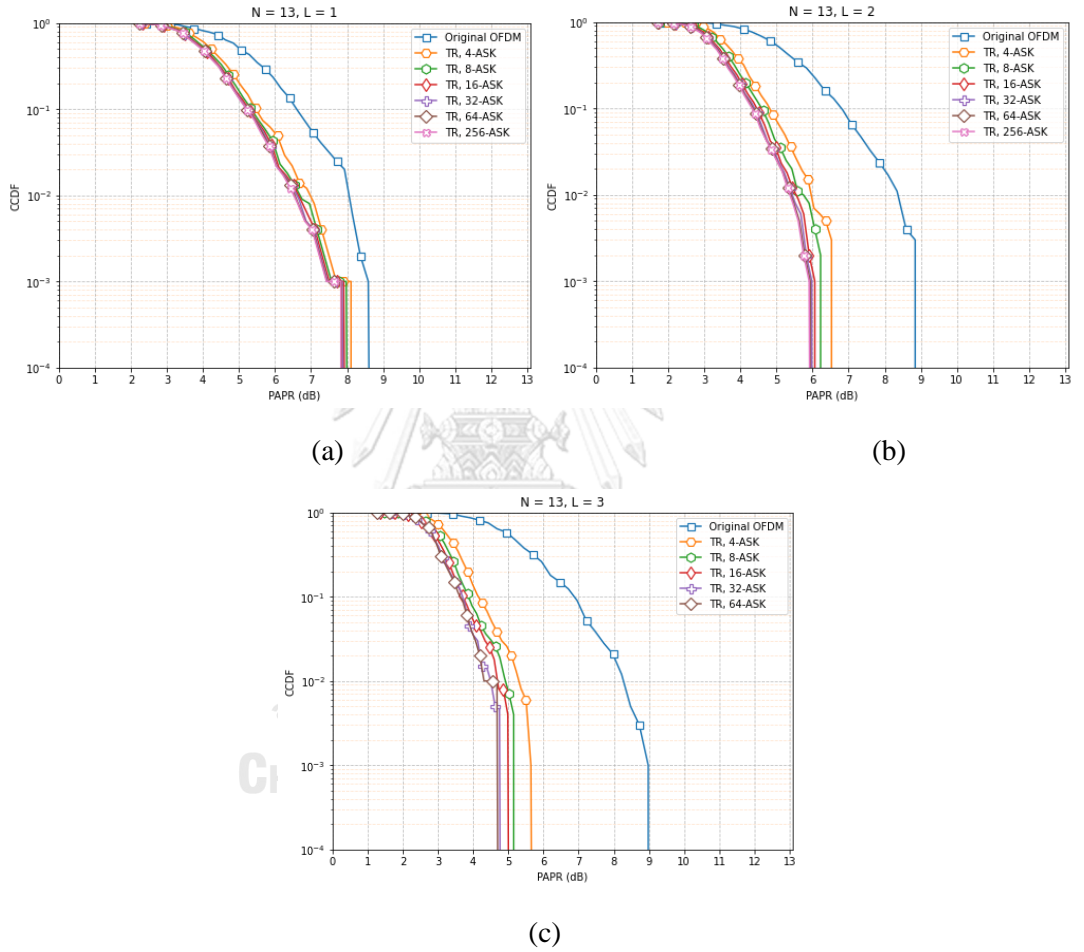


Figure 19. CCDF vs PAPR curves for TR, M-ASK, at  $N = 13, L = 1, 2, 3$

### M-QAM canceling tones:

The M-ary Quadrature Amplitude Modulation (M-QAM) signal constellation is defined as shown by eq.(4.3):

$$s_k = \sqrt{\frac{3E_c}{2(M-1)}} \left[ (2 \times m + 1 - \sqrt{M}) + j(2 \times n + 1 - \sqrt{M}) \right], \quad m, n = 0, 1, 2, \dots, \sqrt{M} - 1 \quad (4.3)$$



where  $E_c$  is the average energy per canceling signal. Figure 17(c) shows the signal constellation of the canceling signals in the frequency domain for  $M = 4, 16, 64,$  and  $256$ . Unlike, the M-PSK where only phases varied, and M-ASK where only amplitudes varied, M-QAM offers various combinations of both phases and amplitudes in the canceling signals. Our simulation results as shown in Figure 20 have confirmed that such variations in amplitudes and phases of M-QAM are beneficial for PAPR reduction, as the PAPR reduction gains achieved by M-QAM are always better than the other two when  $M$  is greater than 4. It appears also that like M-PSK and M-ASK, the PAPR reduction gains can be improved by increasing the number of canceling tones, although the improvement by M-QAM is more prominent. For instance, at  $\text{CCDF}=10^{-3}$ , the 16-QAM approximately achieves the gains of 1.5 dB, 3 dB, 3.5 dB with reference to original OFDM for  $L = 1, 2, 3$  respectively. When the number of signal candidates is increased from  $M = 4$  to  $M = 16$ , the PAPR reduction gains are noticeably improved. However, further increases in the number of canceling signals candidates to 64-QAM and 256-QAM provide much fewer improvements in PAPR reduction gains.

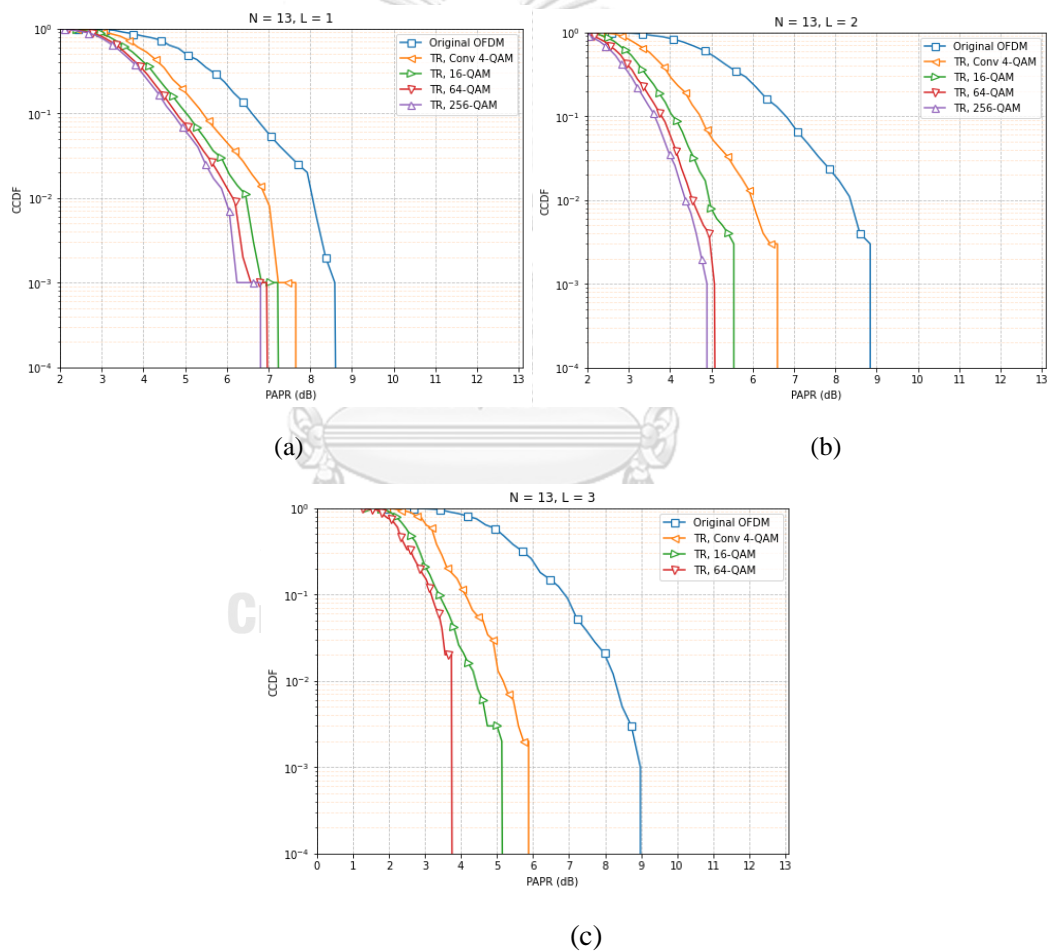


Figure 20. CCDF vs PAPR curves for TR, M-QAM, at  $N = 13, L = 1, 2, 3$

Table 4. Computational time requirements of TR for different signal constellations with 1000 OFDM samples and  $N = 13$

(a) M-PSK

$M$	Computational time, $T$ (seconds)		
	$L=1$	$L=2$	$L=3$
4	2.4	8.1	17.7
8	3.4	30.2	141.7
16	5.4	117.8	1125.9
32	8.8	449.5	9099.0
64	15.9	1434.4	71083.0
256	59.5	18408.3	NA

(b) M-ASK

$M$	Computational time, $T$ (seconds)		
	$L=1$	$L=2$	$L=3$
4	2.9	5.5	32.3
8	4.0	17.6	214.1
16	5.3	119.5	1127.7
32	12.3	262.4	8727.0
64	16.8	1023.6	73628.0
256	63.3	16570.1	NA

(c) M-QAM

$M$	Computational time, $T$ (seconds)		
	$L=1$	$L=2$	$L=3$
4	2.4	10.6	19.1
16	5.2	124.7	1132.2
64	16.4	1804.3	80929.5
256	62.1	18878.4	NA

Table 4 summarizes the actual computational time requirements for TR when using different M-PSK, M-ASK, and M-QAM signal constellations. The computer used in the experiments has the following specifications: Windows 10, Intel Core i7-1065G7, RAM: 8 GB, GPU is not used in the experiment. The numerical results show that the actual computational time of M-PSK, M-ASK, and M-QAM measured in seconds all increase with the number of canceling signal candidates, which is equal to  $M^L$ . For small values of  $M$ , i.e., 4 and 16, the CCDF curves can be obtained swiftly for  $L = 1$ , under 2 minutes for  $L = 2$  and under 20 minutes for  $L = 3$ . As the values of  $M$  are increased to 64 with  $L = 3$ , the computational time required is almost one day. When  $M = 256$  and  $L = 3$ , no results are obtainable in a reasonable time, as the estimated time to get the CCDF curve is 47 days. Therefore, to ensure that the proposed TR-based PAPR reduction technique can be applied in practice, it is necessary to focus on  $M = 16$ , because of the computational time constraint for real-time transmission of OFDM signals. In addition, at  $M = 16$  as discussed earlier, M-QAM shows promising potentials to attain high PAPR reduction gains.

## 4.2. Modified Peak Canceling Tones Mapping Using PSO with TR

As we have seen above that variation in the mapping of QAM level from QAM-4 to QAM-256 gives some prominent PAPR reduction. Therefore, we have selected to modify the canceling tone candidates of QAM-16 with the use of the Particle Swarm Optimization (PSO) technique. Because it gives 0.5 dB better PAPR gain in contrast to the conventional QAM-4. There are other higher QAM levels such as QAM-64 and QAM-256 which we did not consider using since QAM-64 and QAM-256 provide 0.2 dB and 0.4 dB, respectively in contrast to QAM-16 at the cost of very high computational time which makes them very difficult to use. Before we explain our proposed TR-based PSO methodology, we first wanted to find out which type of canceling tones are most frequently used in contrast to other tones. Figure 21 shows our results regarding this.

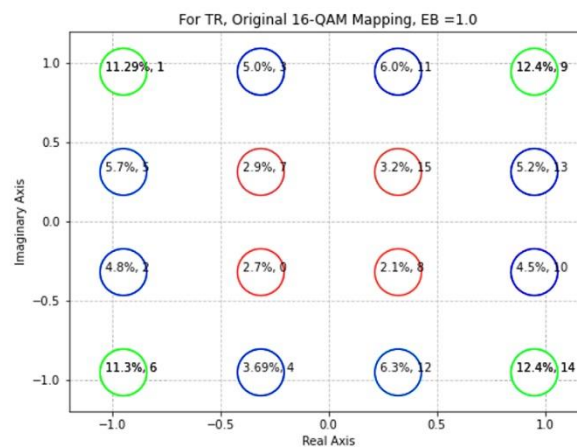


Figure 21. Distribution of canceling tones used for PAPR reduction

Figure 21 shows that only the canceling tones marked with green circles in the 4 corners of 16-QAM mapping are utilized the most as they overall have a usage of 48% in contrast to the other QAM-16 canceling signals. We have also seen that each of these corner candidates is also being utilized by the TR by equal proportions, so we grouped them as one class of canceling tones. The second group that we consider is the 8 blue circles beside the green corner canceling candidates have the next highest total proportions of 41%. They also carry almost equal percentages of occupancy among themselves. The third group has a total proportion of 11% which is the lowest among all the groups. This indicates that the 4 red canceling tones in the center are the least frequently used.

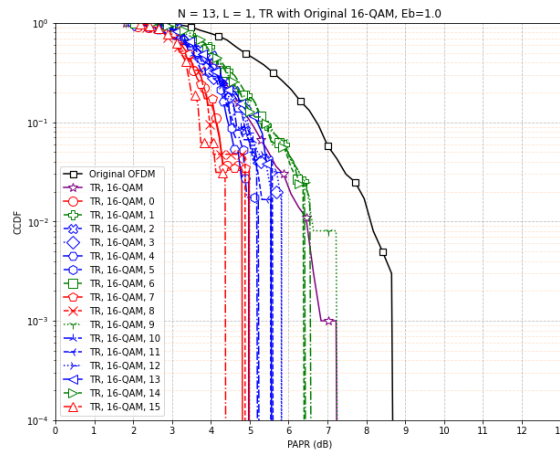


Figure 22. CCDF distribution of each canceling tone of QAM-16

Figure 22 demonstrates that the 3 groups of canceling tones that we have distinguished above show similar CCDF. The corner canceling candidates in green circles have almost the same CCDF characteristics. As well as the 4 canceling candidates in the middle, and the rest of the 8 canceling candidates also have similar PAPR characteristics as shown by the red and blue curves, respectively in Figure 22. This also depicts that the outer canceling candidates represented by the blue and green circle in Figure 21 dominate the overall CCDF distribution of TR with QAM-16 which is represented by the purple curve in Figure 21. This happens because the 2 groups in the outer circle are more frequently used than the other group in the middle of the inner circle.

Since we know from Figure 21 that the canceling candidates in the corner have the highest proportions for reducing PAPR, therefore we try to amplify the corner signals in such a way that the overall average energy per signal of the canceling signals remains close to 1. Since we have seen that if we increase the average energy of canceling candidates to be too high, they incur a negative effect on the signals by distorting them and increasing their BER. As a result, we must adjust our canceling candidates in such a way that they don't result in additional distortions to the OFDM signal. However, it is very difficult to be able to manually change the canceling candidates such that the overall average,  $E_c$ , always remains precisely to 1. Therefore, we used the Particle Swarm Optimization (PSO) to find a better combination of canceling signal candidates for providing a better gain in PAPR with the same average energy per signal.

Particle swarm optimization (PSO) [39] is a type of optimization technique that is highly prominent in finding proper optimization for un-convex, un-continuous and large dimensional problems. It is a simple technique that does optimization based on flocking or schooling of birds or fishes, which is a natural process. The PSO constantly maintains a balance among 3 different pulling forces on each of its particles which helps to maintain the best group location,  $p_k^g$ , and the best position of each individual particle,  $p_k^i$ , at each iteration,  $k$ , causing the particles to swarm in one direction as shown by Figure 23. These 3 forces are named as follows:

- a) Inertia: The force due to the particles' previous velocities.
- b) Cognitive Force: The force due to an individual particle's distance from the best-known location.

- c) Social Force: The force due to the swarm's best position known at a moment.

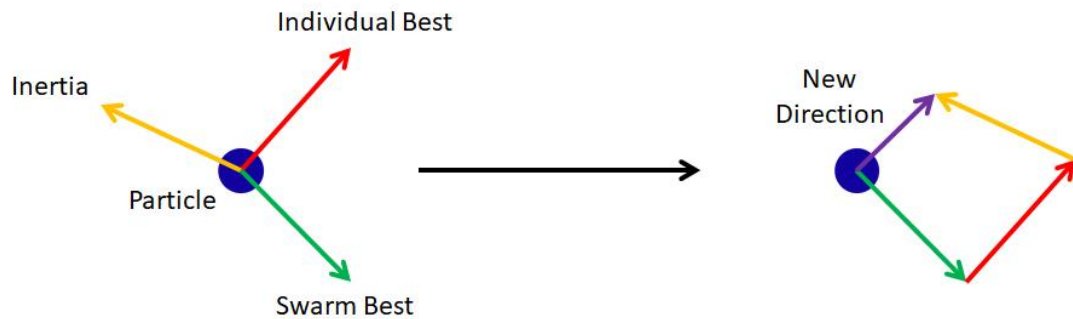


Figure 23. Particle Swarm Optimization [39]

In PSO, the position and velocity of particles are defined by eq.(4.4.a), and eq.(4.4.b) and as shown below:

$$v_{k+1}^i = w_k v_k^i + c_1 r_1 (p_k^i - x_k^i) + c_2 r_2 (p_k^g - x_k^i) \quad (4.4.a)$$

$$x_{k+1}^i = x_k^i + v_{k+1}^i \quad (4.4.b)$$

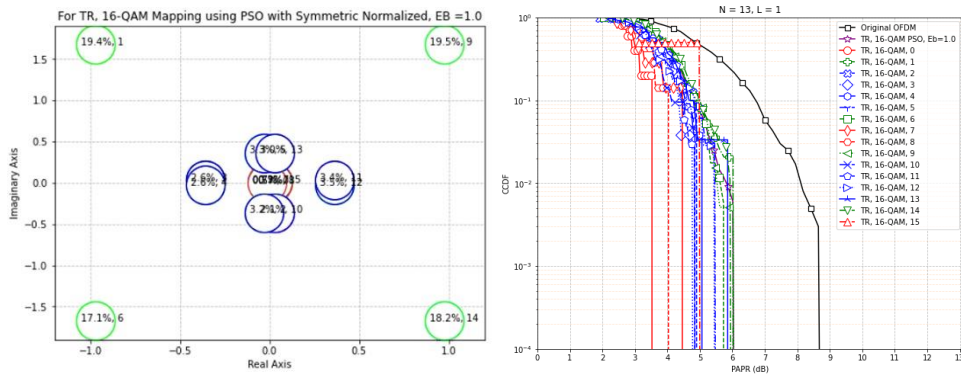
In eq. (4.4.a),  $w_k$  is the constant inertia weight for all  $k$  iterations,  $c_1$  is the cognitive constant,  $c_2$  is the social constant,  $r_1$  and  $r_2$  are numbers which are random in nature between 0 to 1,  $p_k^i$  is the best known individual  $i$ -th particle position at the  $k$  iteration,  $p_k^g$  is the best group position of the particles at the  $k$  iteration and  $x_k^i$  represents the position of the  $i$ -th particle at the  $k$  iteration. Based on the magnitudes of  $c_1, c_2, r_1, r_2, p_k^i, p_k^g$ , and  $x_k^i$  two important terms are calculated which is the social term, i.e.  $c_1 r_1 (p_k^i - x_k^i)$  and the cognitive term, i.e.  $c_2 r_2 (p_k^g - x_k^i)$  for the  $i$ -th particle at the  $k$  iteration. By adding the magnitude of  $w_k v_k^i$  to the social term and the cognitive term provides the new velocity of the  $i$ -th particle at the  $k+1$  iteration as shown in eq. (4.4.a). And after this, the new position,  $x_{k+1}^i$ , of the  $i$ -th particle can be found by adding the new velocity,  $v_{k+1}^i$ , at  $k+1$  iteration to the old position of the  $i$ -th particle at the  $k$  iteration as shown in eq. (4.4.b). From these two equations the algorithm of PSO is shown below as follows:

1. The following initializations must be done before the PSO starts:
  - a) The constants are set as follows: the total number of iterations the PSO is allowed to run is set to  $k_{\max}$ , the total number of particles is set to  $n$ ,  $w_k$  is set to 0.5,  $c_1$  is set to 1, and  $c_2$  is set to 2. The magnitudes of  $c_1$  and  $c_2$  normally range from 0.5 to 2.5. Here,  $c_2 > c_1$  so that the PSO particles are strongly captivated to move towards their highest accurate group positions during optimization.
  - b) Set the positions  $p_k^i$  of the  $i$ -th particles, randomly.

- c) Find the best-known position of the swarm,  $p_k^g$  at  $k = 1$
- d) Set the velocities  $v_k^i$  of the  $i$ -th particles randomly.
- e) Set  $k = 0$  for counter iteration.
2. Optimization is done in the following steps:
  - a) Select  $r_1$  and  $r_2$  randomly in the range of 0 to 1 at each  $k$  iteration.
  - b) Evaluate the cost function  $f(x_k^i)$  for the position,  $x_k^i$  of each  $i$ -th particle at each  $k$  iteration.
  - c) Evaluate the cost function  $f(p_k^i)$  for the best-known individual  $i$ -th particle position i.e.,  $p_k^i$ , at the  $k$  iteration.
  - d) Evaluate the cost function  $f(p_k^g)$  for the best group position of the particles, i.e.,  $p_k^g$  at the  $k$  iteration.
  - e) If  $f(x_k^i) < f(p_k^i)$ , then  $f(p_k^i)$  is set to  $f(x_k^i)$  and  $p_k^i = x_k^i$ .
  - f) If  $f(p_k^i) < f(p_k^g)$ , then  $f(p_k^g)$  is set to  $f(p_k^i)$  and  $p_k^g = p_k^i$ .
  - g) Update the velocities,  $v_{k+1}^i$ , and positions,  $x_{k+1}^i$ , of all the particles at each  $k$  iteration.
  - h) Repeat the above procedure and keep on incrementing  $k$  as long as  $k$  does not reach  $k_{\max}$ . If  $k$  reaches  $k_{\max}$  then the PSO terminates and goes to step 3.
3. When the PSO's algorithm is terminated, the PSO returns the particle that achieves the best near-accurate solution with the lowest value of the cost functions mentioned above.

So using the PSO proposed above we find a fixed set of efficient peak canceling signals for achieving a good PAPR reduction gain for OFDM signals with  $N = 13$  data subcarriers. The PSO that we have used is set to produce symmetric canceling signals which are normalized such that the  $E_c$  is 1. We start from the initial canceling tone candidates of the 16-QAM so that the PSO algorithm converges faster. Since we have already seen before that certain groups of canceling signals have the same CCDF characteristics, we, therefore, have divided the 16 classes of canceling signals into 3 groups. Two of these groups contain 4 candidates each and only one of them contains 8 canceling tone candidates. Since we have also seen that the PSO cannot take complex numbers as inputs, therefore we have divided a canceling tone into separate real and imaginary numbers. As a result, the PSO is given 6 inputs for the 3 classes of canceling tones. And for the output cost function, we have set it as the maximum PAPR of the total OFDM signals in a finite sample size, which the PSO tries to reduce with each iteration. But we allow the PSO to choose freely in the range of -40 to 40 in both the x and y-axis since it is eventually normalized in our PAPR cost function program. We give such a large range for the PSO so that it can choose the canceling tones more accurately with high precision. We also assign the PSO to use  $n = 15$  particles and we also allow the PSO to iterate each of its particles 20 times to find the best minimum PAPR by setting  $k_{\max} = 20$ . In this experiment, we plan to evaluate our TR with PSO in terms of PAPR reduction gain with the help of CCDF vs PAPR curves.





(a) Distribution of canceling tones (b) CCDF distribution of each canceling tone

Figure 24. Distribution of canceling tones using PSO with the symmetric and normalized concept.

Figure 24(a) shows that the total proportions of canceling tones for the corner candidates increase even higher to 74% due to the usage of the PSO with the normalized and symmetric concept in contrast to the other 12 candidates. This gives the corner signals in green circles even higher dominance on the overall CCDF result of TR with 16-QAM modified by the PSO. As a result, the PSO obtained a better minimum PAPR of 6.18 dB keeping the overall  $E_c$  of the canceling tones equal to 1. Figure 24(b) also shows that the green curves resulting from the group of canceling tones with green circles which are most frequently used by the TR have shifted more to the left in contrast to the original 16-QAM discussed above. As a result, the overall purple curve of the TR with PSO has achieved a high PAPR gain in contrast to other techniques mentioned before.

Below is our result of the fitness curve of the PSO for reducing the maximum PAPR as shown in Figure 25. It shows that the maximum PAPR rapidly decreases with a high gradient at the start. But as soon as the PSO reaches higher iterations the Maximum PAPR reaches saturation with a local minimum value of the maximum PAPR.

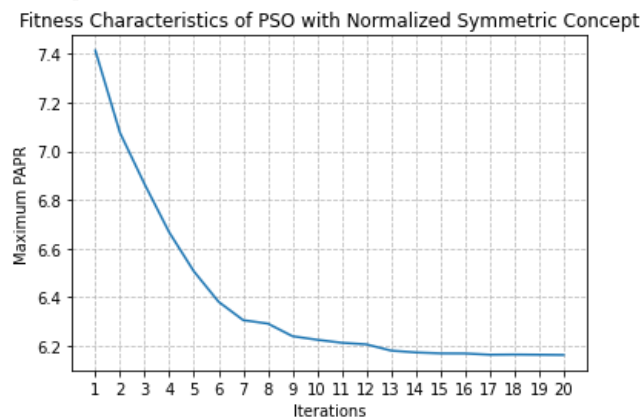


Figure 25. Fitness characteristics of PSO

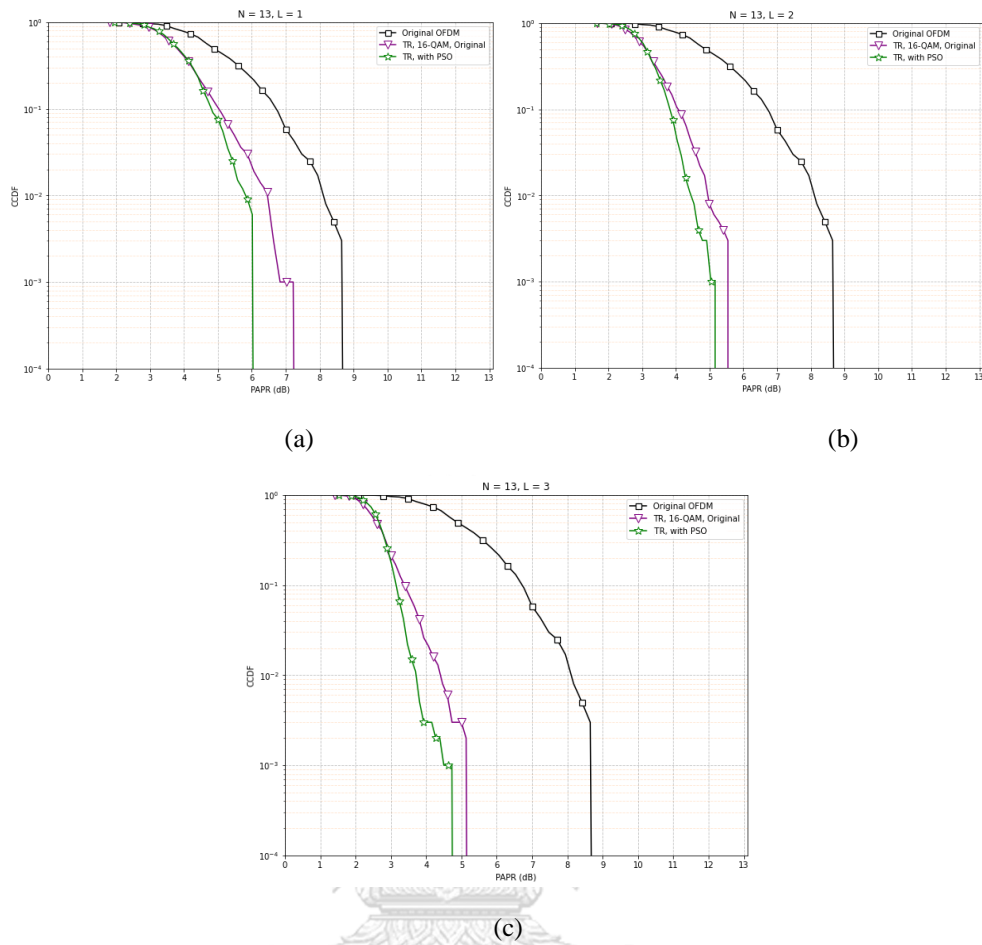


Figure 26. CCDF curves for comparison of PSO with and original QAM-16 at  $L = 1, 2, 3$

Figure 26(a) to Figure 26(c) shows the CCDF distribution of the PSO compared to the original QAM-16 candidates for use in TR. We can see an overall increased gain of approximately 0.5dB for the PSO in contrast to the original QAM-16 candidates which we could predict systematically since we kept the constraint of  $E_c = 1$  for  $L = 1, 2, 3$ . If we kept a higher magnitude of  $E_c$  we probably can predict that the gain in PAPR reduction will be higher, but adversely the BER may also be higher due to the uneven distribution of energy per signal ( $E_c$ ) for an OFDM signal.



## Chapter 5: Experiment and Discussion

In section 5.1 of this chapter, the TR with PSO is first evaluated in terms of PAPR reduction and computational time, when the total number of canceling signals is carefully reduced from 16 to 8 canceling signals. The objective of this evaluation is to find out whether the carefully chosen 8 canceling tones from the TR-based PSO provide the same CCDF vs PAPR curves as the original TR-based PSO with 16 canceling tones. Then in section 5.2 further experimentations are carried out to evaluate TR-based PSO with and without the usage of generic classifiers. The objective of this section is to find out whether the use of classifiers aids the TR-PSO to reduce its computational time further while maintaining the same PAPR reduction performance. Finally, in section 5.3 all the PAPR reduction techniques mentioned in Chapter 3 are compared with the proposed TR-PSO to evaluate its overall performance in terms of PAPR and computational time.

### 5.1. Evaluation of TR-PSO:

As per the first objective of this chapter, we first select the 8 canceling signal candidates from the 16 canceling signal candidates provided by the PSO shown in Figure 24(a) above. We directly choose the 4 candidates in the corner shown by the green circle in Figure 24(a) previously and Figure 27 below. For obtaining the other 4 candidates we use the inner 8 circles represented in blue in Figure 24(a) and we take an average of the closest two consecutive canceling signal candidates represented in blue and finally, we get the other 4 canceling signal candidates which are also shown in blue color in Figure 27 below.

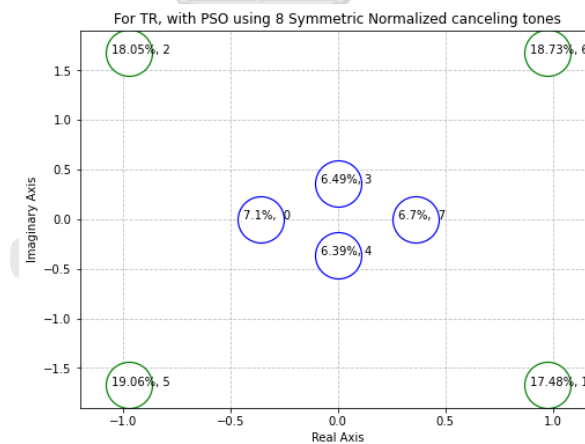


Figure 27. Distribution of 8 canceling tones

As the 8 canceling tones have been already selected then we set up an experiment to test these chosen 8 canceling signal candidates on OFDM signals with  $N = 13$  subcarriers to see whether the frequency of using the canceling tone candidates by the TR has changed or not. Furthermore, we would also like to evaluate whether the PAPR performance and computational time of our proposed TR-PSO changes with the reduction in the total number of canceling signal candidates from 16 to 8. The experiment is carried out on a computer with the following setting: Windows 10, Intel Core i7-1065G7, RAM: 8 GB, GPU is not used in the experiment. The samples of random OFDM signals used in the experimentation has mean of 0.25 and variance of 0.011 and its PDF can be demonstrated as shown below:

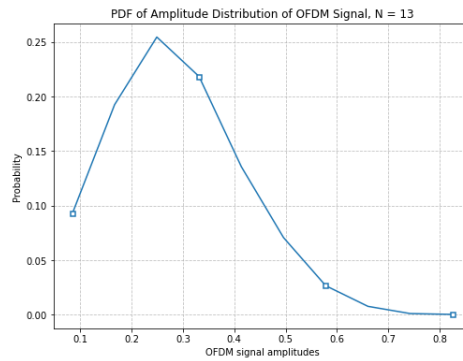


Figure 28. PDF of OFDM signals with  $N=13$  subcarriers

From our experiment, we observe that the corner candidates have the same overall proportion (%) of usage as approximately 74% as they had before and the rest of the 4 candidates take over the remaining 26%. Since the corner candidates are the most dominating, so the overall CCDF versus PAPR curve of the TR with PSO with 8 candidates remains exactly similar to the original TR-PSO with 16 candidates at  $L=1,2,3$  canceling tones as shown below in Figure 29. As per the results of this experimentation, we can use our chosen 8 candidates for representing our proposed TR with PSO instead of the 16 candidates that we did earlier.

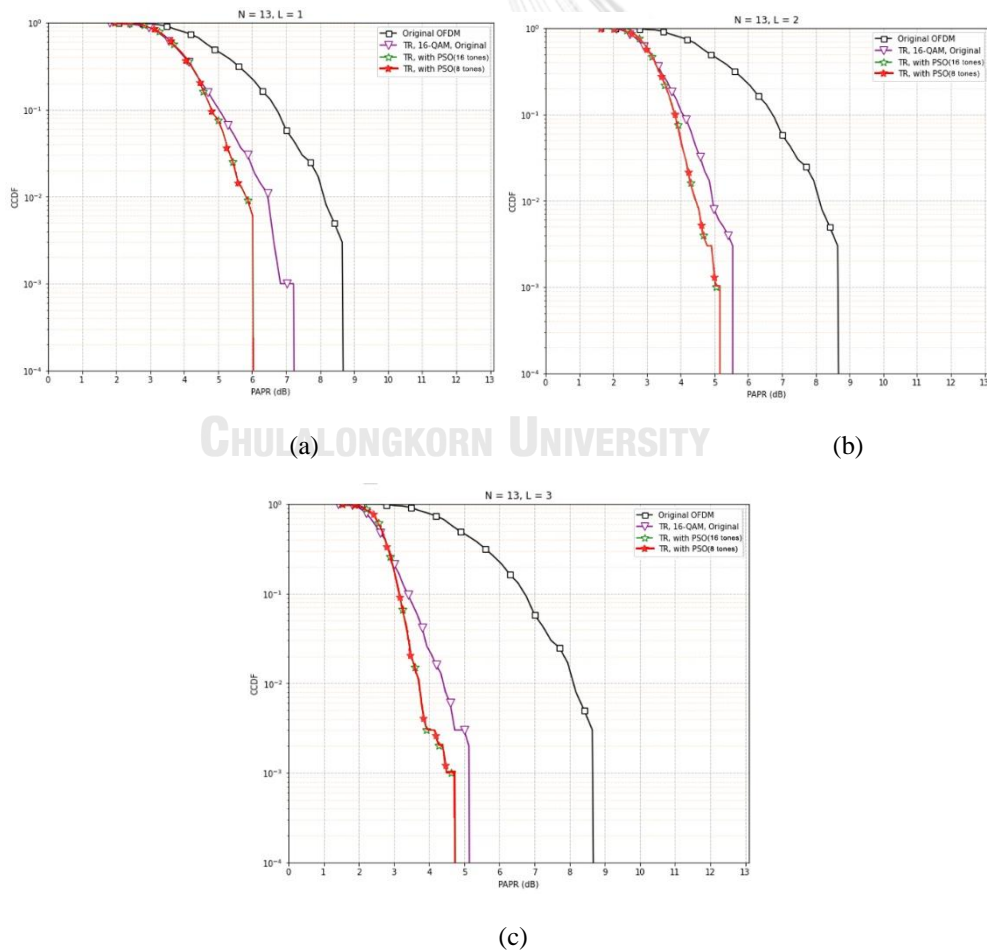


Figure 29. CCDF curves for comparison of PSO with and original QAM-16 at  $L = 1, 2, 3$

Table 5. Computational time requirements of TR with PSO at  $L = 1,2,3$ , for 1000 samples,  $N = 13$

Technique	Computational Time, T (seconds)		
	$L=1$	$L=2$	$L=3$
TR with PSO (16 candidates)	5.2	124.7	1132.2
TR with PSO (8 candidates)	3.4	30.2	141.7

Table 5 shows the computational time requirements for our proposed TR-PSO with 8 and 16 canceling signal candidates. It clearly shows that the computational time has decreased by almost 8 times for TR-PSO with 8 candidates at  $L = 3$  in comparison to TR-PSO with 16 candidates while maintaining the same PAPR reduction performance.

## 5.2. Evaluation of TR-PSO with classifiers:

As per the second objective, we want to evaluate TR-based PSO with and without the usage of some classifier models. There are many available classifiers such as Perceptron, Naive Bayes, Decision Tree, Logistic Regression, K-Nearest Neighbour, Artificial Neural Networks (ANN), Support Vector Machine. For fulfilling this objective, we will combine the ANN classifier models with our proposed TR-PSO PAPR reduction technique. Furthermore, we plan to combine two types of ANN models with our proposed TR-PSO. The first ANN model is named the binary ANN classifier which will be used to classify the high and low PAPR OFDM signal classes based on a set hard threshold PAPR level. The second ANN model is named the multiclass ANN classifier which will be used to classify the peak canceling signals used by the TR-PSO. The objective of this section is to find out whether the use of a combination of the ANN classifiers aids the TR-PSO to reduce its computational time further while maintaining the same PAPR reduction performance.

So to evaluate the TR-PSO with the classifiers mentioned above we set up an experiment on OFDM signals with  $N = 60$  subcarriers and  $D = 30$  dummy subcarriers. The OFDM signals used in this experiment have mean of 0.084 and variance of 0.0039 and its PDF is shown in Figure 30 below.

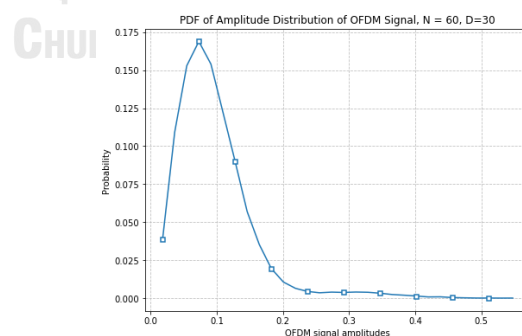


Figure 30. PDF of OFDM signals with  $N = 60$  data subcarriers and  $D = 30$  dummy subcarriers

In this experiment, the TR-PSO with and without classifiers will be evaluated in terms of their PAPR reduction performance, computational time, and average test accuracies. The experiment will be conducted on 5 different sets of OFDM data signals and the final test accuracy will be calculated as an average of the 5 different test accuracies with the same setting of training to testing ratio to 0.8:0.2 each time for both the binary and the multiclass ANN

modules. The experiment is carried out in a computer with the following configuration: Windows 10, Intel Core i7-1065G7, RAM: 8 GB, GPU is not used in the experiment.

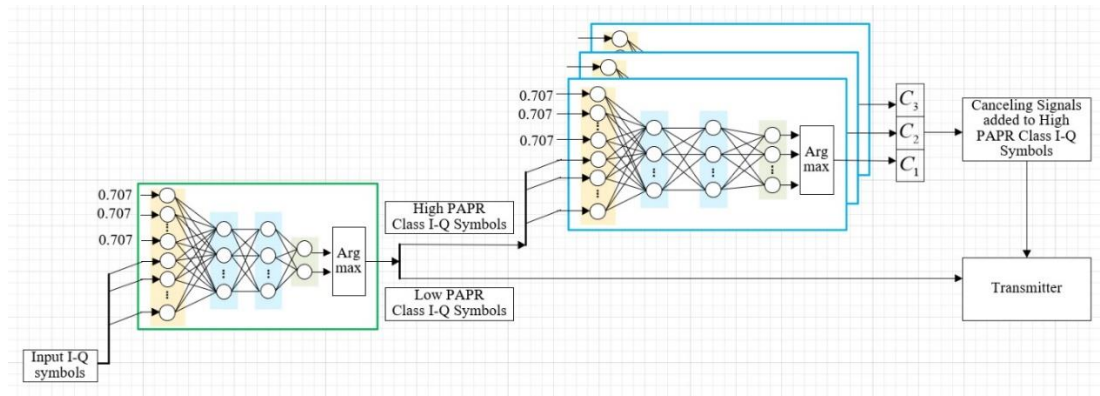


Figure 31. Model of binary class ANN and multiclass ANN with the TR-PSO

So now to fulfill the second objective of this section we first design an ANN model that consists of a binary ANN classifier model [40] connected serially to a multiclass parallel ANN classifier model and a transmitter as shown in Figure 31 above. Our designed binary class ANN classifier module consists of 4 fully connected layers (1 input layer, 2 hidden layer and 1 output layer). The input consists of 180 neurons with each neuron receiving input data sizes of 180 in shape. In this experiment, we want to train our binary class ANN module for  $N = 60$  data subcarriers which have an equivalence of  $2^{N \times B} = 2^{60 \times 2} = 1.3 \times 10^{36}$  different combinations of input frequency domain (I-Q) data patterns. Moreover, we would also like to add  $D = 30$  dummy sub-carriers inputs at the front of the data subcarriers for easy training of the binary class ANN module. The 1<sup>st</sup> and 2<sup>nd</sup> hidden layers consist of 8 neurons each. The output hidden layer consists of 2 neurons for giving the output for 2 different classes of high PAPR and low PAPR OFDM signals as labels which are represented by a one-hot encoding. And then argument max function is used to determine the predicted label of the input OFDM signals regarding whether it belongs to the high or low PAPR class of OFDM signals. After the prediction has been made, the low PAPR OFDM signals in the frequency domain are directly sent to the Transmitter block for processing them for transmission as shown above in Figure 31[40].

And in the case of the high PAPR OFDM signal classes, they will be sent to our Parallel model of multiclass ANN module for processing these high PAPR OFDM signals further for reducing their PAPR. The model of multiclass ANN classifier model that we have designed is a sequential model consisting of 4 fully connected layers (1 input layer, 2 hidden layer and 1 output layer). The multiclass ANN module will also be trained for  $N = 60$  subcarriers for the high PAPR OFDM signal classes only. We also add  $D = 30$  dummy sub-carriers inputs at the front of the data subcarriers for easy training of the multiclass ANN module. The input consists of 180 neurons with each neuron receiving input data sizes of 180 in shape. The hidden layers consist of 8 neurons each. The output hidden layer also consists of 8 neurons for the output of 8 different classes of peak canceling signals which are represented by a one-hot encoding. And then argument max function is used to determine the predicted label of the canceling tone. Afterward, the canceling signals will be combined with the high PAPR OFDM signal classes in another block and then they will be finally sent to the Transmitter block for processing them for transmission as shown in Figure 31. Both of our binary class and multiclass ANN modules use Adam as their optimizer. We have also kept some other parameters as constants for both of

them such as the learning rate is taken as 0.01, the number of epochs is taken as 2 for the binary classifier and as 5 for the multiclass classifier. Moreover, the training to testing ratio is kept as 0.8:0.2, and activation function of the input, hidden and output layers is taken as Sigmoid.

For training the binary ANN classifier module, we set 11 dB as the hard threshold PAPR and any input signal with PAPR above this threshold is considered to have high PAPR. For setting 11 dB as the hard threshold PAPR, the proportion (%) of the high PAPR problem in the total sample size of 10000 OFDM signals becomes 40%. The average test accuracy we obtain from using our binary ANN classifier on 5 different sets of I-Q frequency domain input signal is 98.0%. For our multiclass ANN module, the average test accuracies that we get for separately training each canceling signal:  $C_1, C_2$  and  $C_3$  for  $L = 1, 2, 3$  canceling signals are shown in Table 6. It depicts that we achieve an overall average test accuracy of 95% for using our Parallel model of multiclass ANN module for all the tested values of  $L$  canceling signals.

Table 6. Test accuracy of multiclass ANN for TR-PSO at  $N = 60$  and  $L = 1, 2, 3$  for 10000 samples

Total number of Canceling signals ( $L$ )	Test Accuracy (%)		
	$C_1$	$C_2$	$C_3$
1	95.1	-	-
2	95.5	95.2	-
3	95.6	95.3	95.1

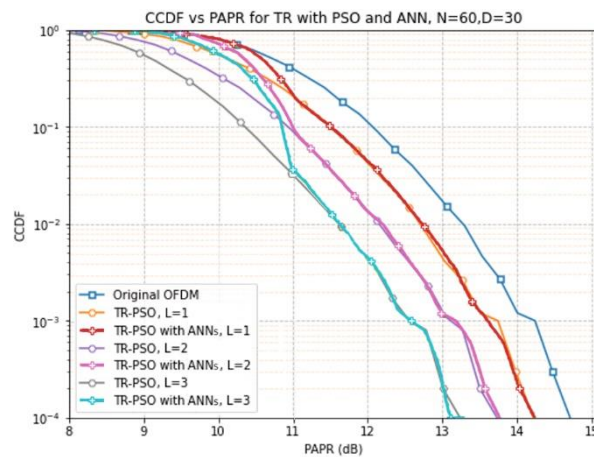


Figure 32. CCDF vs PAPR curves for TR-PSO with and without ANNs for  $L = 1, 2, 3$

Figure 32 shows the CCDF vs PAPR curves for TR with original PSO having 8 candidates with and without ANNs for  $L = 1, 2, 3$  canceling signals. It is clearly seen that when we use a binary class ANN module combined with our TR with PSO with 8 candidates, there seems to be an increase in CCDF of any PAPR below 11 dB. This happens because 11 dB was set as the threshold PAPR for the binary classification of high and low PAPR signals. As a result, any OFDM signal having PAPR lower than 11 dB such as an OFDM signal having a PAPR of 10 dB is considered as low PAPR OFDM signals and so are not processed for PAPR reduction as a result they remain unchanged. When PAPR is greater than 11 dB, i.e., suppose an OFDM signal having a PAPR of 12 dB is processed for PAPR reduction with  $L = 3$  reserved



signals, its PAPR value may reduce to a magnitude of 10 dB. As a result, the CCDF of OFDM signals having PAPR = 10 dB will increase. So, in general, the OFDM signals that have PAPR lower than any chosen threshold PAPR set for the binary ANN classifier will see a rise in its CCDF below the threshold value. But above the threshold PAPR level of 11 dB, the TR-PSO without ANN and the TR-PSO with ANNs approximately overlap. Moreover, since our proposed model of combined ANNs also has an overall average test accuracy of 95% and therefore the PAPR reduction performance of the combined ANNs almost overlaps exactly with that of the TR-PSO without ANNs. This proves that our proposed combination of ANN models with TR-PSO can successfully achieve the same PAPR reduction performance with just 8 canceling candidates when compared to the TR-PSO without ANNs for any value of  $L$  canceling signals. Moreover, using TR-PSO with the combination of binary and multiclass ANN classifiers also reduces the computational time of the processing of the OFDM signals for PAPR reduction greatly as shown in Table 7 below.

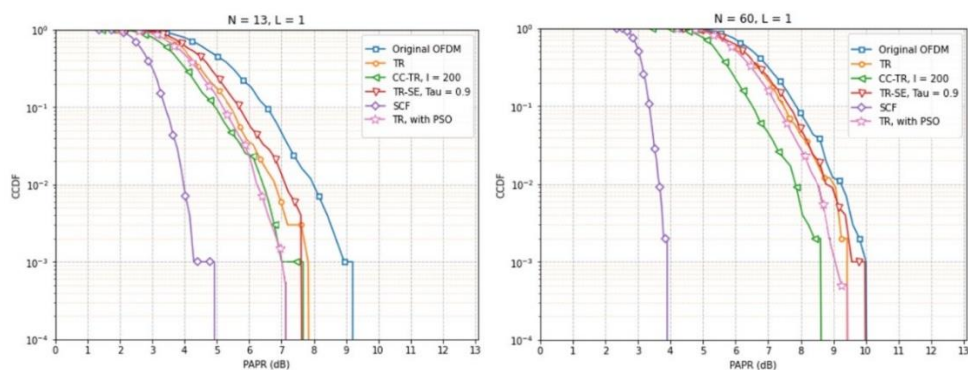
Table 7. Computational time requirements of TR with PSO at  $L = 1, 2, 3$  for 10000 samples,  $N = 60$

Technique	Computational Time, T (seconds)		
	$L=1$	$L=2$	$L=3$
TR-PSO without ANNs	263.1	1191.9	12462.9
TR-PSO with ANNs	5.0	5.0	5.0

Table 7 shows that combining the binary and multiclass ANN classifiers with the TR-PSO with 8 canceling signal candidates reduces the computational time for a given sample of OFDM signals with a very high margin of 98% for any values of  $L$  while maintaining the same PAPR reduction performance as similar to TR-PSO without ANNs.

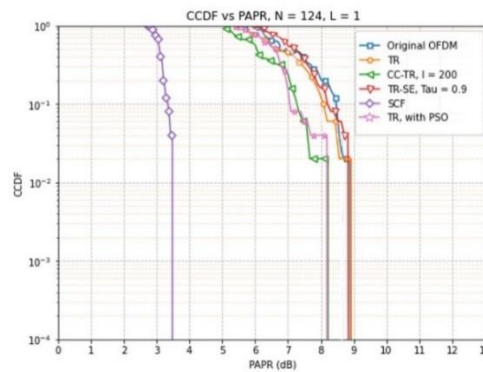
### 5.3. Comparison of PAPR reduction techniques

Finally, in this section, we compare our proposed PAPR reduction technique, TR-PSO with the conventional PAPR reduction techniques i.e. TR, CC-TR, SCF and TR-SE in terms of CCDF vs PAPR curves showing their PAPR reduction gain and computational time as shown below:



(a)

(b)



(c)

Figure 33. CCDF vs PAPR curves for PAPR reduction techniques for  $N = 13, 60, 124$  at  $L = 1$

Figure 33 shows the CCDF curve of original OFDM, TR, CC-TR at  $I = 200$  iterations, TR-SE, SCF, and our proposed PAPR reduction scheme TR-PSO at  $L = 1$  reserved tone for  $N = 13, 60,$  and  $124$  subcarriers, respectively. It is seen in Figure 33(a) that for  $N = 13$  subcarriers, the TR-SE achieves a gain of approximately 1 dB by using its quantized set of candidates having the constraint of a unit energy per signal. The conventional TR also achieves a gain of approximately 1 dB by using its finite set of QAM-4 canceling tones. On the other hand, the CC-TR achieves a gain of approximately 2 dB due to having the highest flexibility in choosing any set of canceling tones that it prefers to attain. But this flexibility comes at the cost of increased computational time which will be discussed later in this section. Interestingly in contrast to TR and CC-TR, we also see that the SCF can attain an even higher gain of PAPR reduction magnitude which is equal to 4 dB. The SCF also does not require any canceling signals like the TR and CC-TR and so SCF has full spectral efficiency. As well as SCF does not also suffer from increased computational time. But there is a major drawback to the SCF's algorithm which is it adds distortion to in-band frequencies of OFDM signals as a result, it heavily increases the BER of a received OFDM signal as shown in [2]. Therefore, even though the PAPR reduction gain is high for SCF, it is not desirable to be used for OFDM systems.

Our proposed technique, TR-PSO provides a finite set of 8 pre-defined candidates with the constraint of overall average energy per signal equal to 1. So the results for our TR-PSO show that it achieves almost 0.5 dB and 1.8 dB greater PAPR reduction gain than the CC-TR, and both the conventional TR and the TR-SE by using just using 1 canceling signal for  $N = 13$  subcarriers. In the case of  $N = 60$  subcarriers which is shown in Figure 33(b), our proposed TR-PSO technique achieve a similar CCDF performance with a higher PAPR reduction gains of 0.1dB, in contrast to the TR with QAM-4 candidates and TR-SE and approximately 0.6 dB in contrast to the original OFDM, respectively. It lags behind the CC-TR by just approximately 0.5 dB. For  $N = 124$  subcarriers, which is shown in Figure 33(c), our proposed TR-PSO has approximately similar CCDF as the CC-TR with 200 iterations at  $L = 1$  and  $N = 124$  subcarriers.

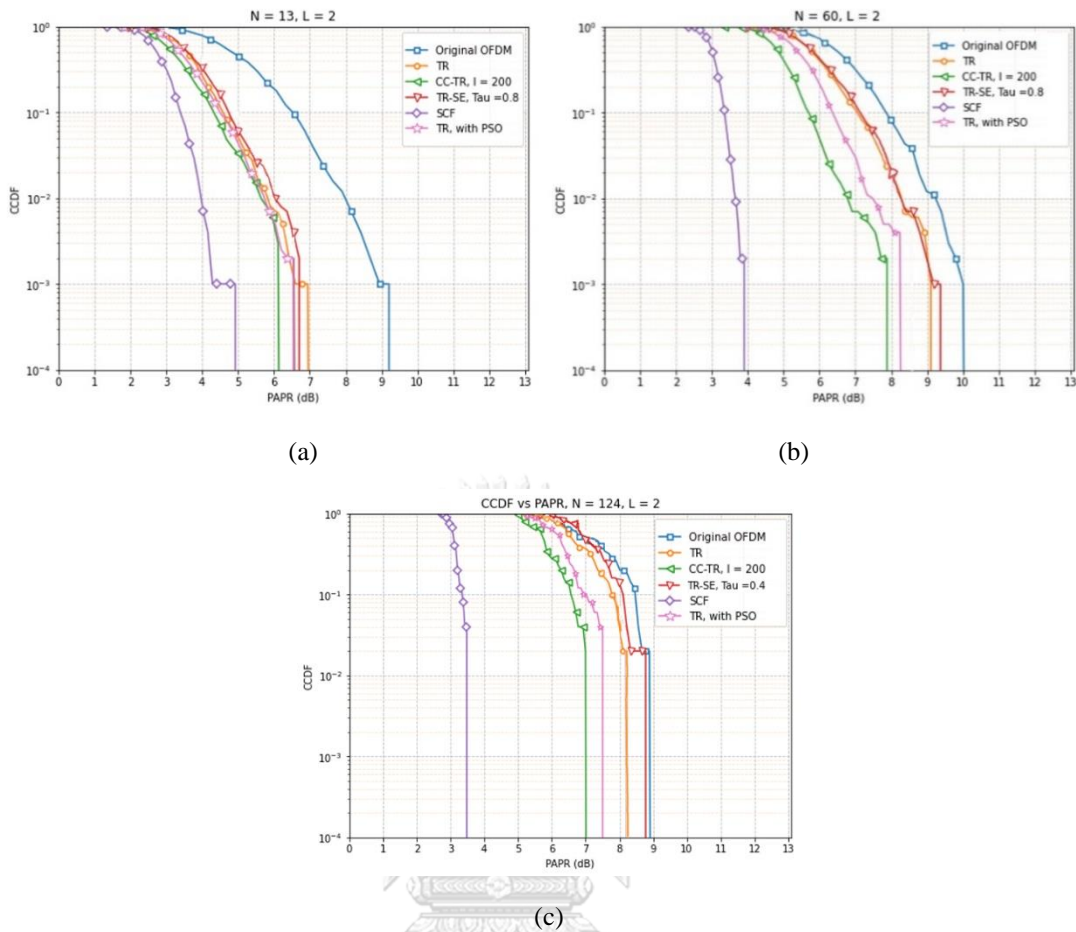


Figure 34. CCDF vs PAPR curves for PAPR reduction techniques, for  $N = 13, 60, 124$  at  $L = 2$

Figure 34 shows the CCDF curve of original OFDM, TR, CC-TR at  $I = 200$  iterations, TR-SE, SCF, and our proposed TR-PSO technique at  $L = 2$  reserved tones for  $N = 13, 60$ , and 124 subcarriers. Figure 34(a) shows that for  $N = 13$  subcarriers, the gain by the TR-SE and conventional TR has increased to approximately 2 dB in contrast to the original OFDM. In the case of CC-TR, it achieves a gain of 3.2 dB and the SCF also achieves a gain of approximately 4.2 dB compared to the original OFDM. Our proposed TR-PSO technique achieves a similar PAPR reduction gain as the CC-TR, and approximately 0.2 dB better PAPR reduction gain than the conventional TR, and TR-SE at  $L = 2$ . In the case of  $N = 60$  subcarriers which is shown in Figure 34(b), our proposed TR-PSO just lags behind the CC-TR by approximately 0.5 dB, but it has a higher PAPR gain of 0.5 dB, in contrast to both the TR with QAM-4 candidates and TR-SE, and our TR with PSO also has 1.2 dB higher PAPR reduction gain compared to the original OFDM at  $L = 2$ . For  $N = 124$  subcarriers, which is shown in Figure 34(c), our proposed TR-PSO technique achieves a higher PAPR reduction gains of 0.5dB, in contrast to the TR with QAM-4 candidates and TR-SE and approximately 1 dB in contrast to the original OFDM, respectively. The TR-PSO just lags behind the CC-TR by approximately 0.5 dB at  $L = 2$ .



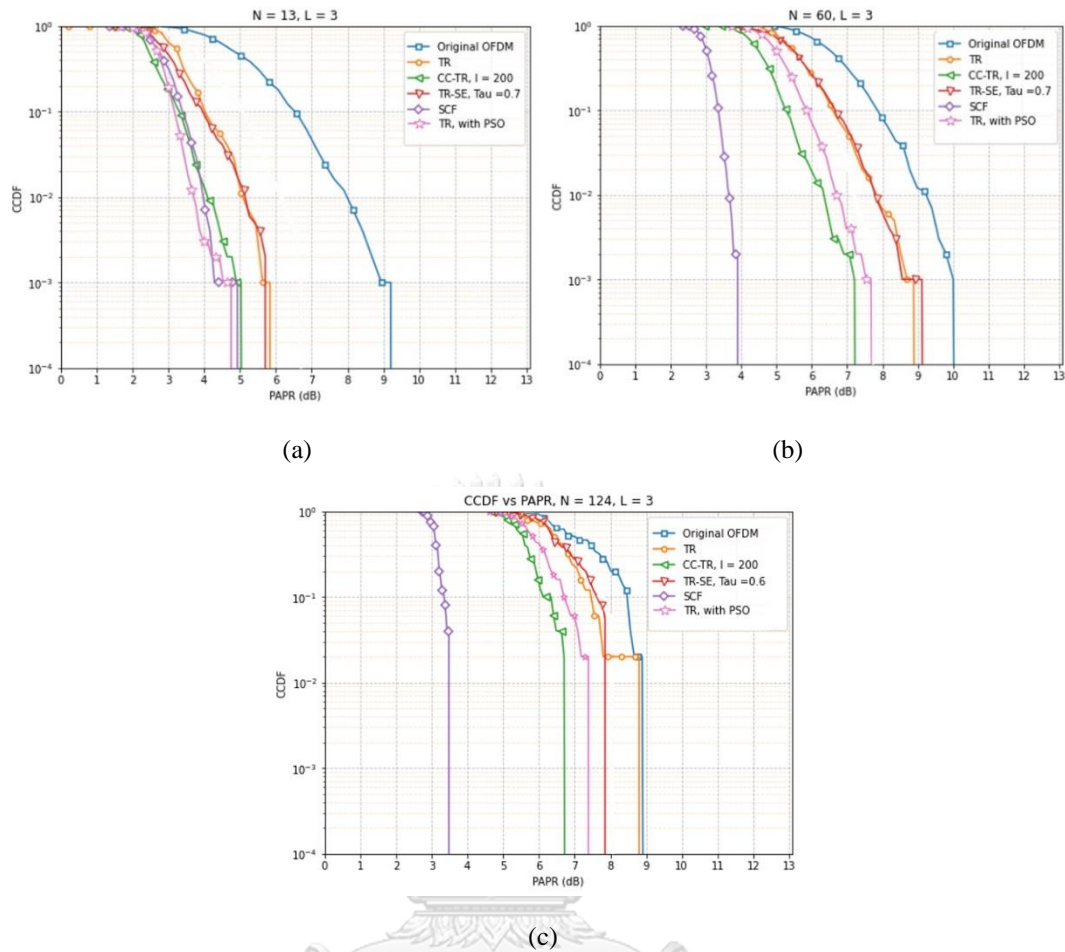


Figure 35. CCDF vs PAPR curves for PAPR reduction techniques, for  $N = 13, 60, 124$  at  $L = 3$

Figure 35 shows the CCDF curve of original OFDM, TR, CC-TR at  $I = 200$  iterations, TR-SE, SCF, and our proposed TR-PSO at  $N = 13, 60,$  and  $124$  subcarriers for  $L=3$  reserved tones. Figure 35(a) depicts that the PAPR reduction gain by the TR-SE and the conventional TR with 4-QAM candidates has increased to approximately 3 dB as well in contrast to original OFDM as well. In the case of CC-TR, it achieves a gain of 4 dB and the SCF also achieves a gain of approximately 4.2 dB. Our proposed TR-PSO achieves a gain of approximately 4.4 dB which is also approximately 0.2 dB, and 1.2 dB, better than the CC-TR, both the conventional TR with 4-QAM candidates and the TR-SE at  $L = 3$ . In the case of  $N = 60$  subcarriers which is shown in Figure 35(b), our proposed S-CC-TR technique achieve a better PAPR reduction gain of 0.5 dB, and 1 dB higher gain in contrast to both the conventional TR with QAM 4 candidates, and TR-SE, and original OFDM, respectively. In the case of TR-PSO, it just lags behind the CC-TR by just approximately 0.5 dB, but it has a higher PAPR gain of 1 dB, and 2 dB in contrast to both the TR with QAM-4 candidates, and TR-SE and the original OFDM, respectively at  $L = 3$ . In the case of  $N = 124$  subcarriers which is shown in Figure 35(c), our proposed TR-PSO just lags behind the CC-TR by just approximately 0.5 dB, but it has a higher PAPR gain of 0.5 dB than the TR with QAM-4 candidates, and TR-SE and approximately 1.5 dB greater PAPR reduction gain than the original OFDM, respectively.

We have also experimented with our proposed techniques and the conventional techniques to find their computational times for different numbers of reserved tones  $L$ . The results of our experiments are shown in Table 8, Table 9 and Table 10 below for  $N = 13, 60$ , and 124 subcarriers, respectively.

Table 8. Computational time requirements of the PAPR reduction techniques at  $N = 13$  and  $L = 1,2,3$ , for 1000 samples

No	Techniques	Computational Time, T (seconds)	Input
			$L$
1	TR	1.1	1
		4.3	2
		17.2	3
2	CC-TR ( $I = 200$ )	44.8	1
		48.6	2
		53.8	3
3	SCF	0.3	-
4	TR-SE	4.2	1
		16.4	2
		51.3	3
5	TR-PSO with ANNs	1.0	1
		1.0	2
		1.0	3

In Table 8, we see that the SCF has the lowest computational time of 0.3s. However, we know that the SCF induces in-band distortion in a transmitted OFDM signal, so it is not often desirable to use. As well as we also see that the TR has a computational time of 1.1 s at  $L = 1$  which increases to 4.3 s and 17.2 s at  $L = 2$  and  $L = 3$ , respectively. This is a predictable observation for TR since higher numbers of  $L$  result in higher combinations of canceling tones,  $M^L$  to be tested by the TR before the best combination of canceling tones that results in the minimum PAPR of a certain OFDM signal is chosen. Therefore, the conventional TR has less priority for use in OFDM systems because it tends to increase its computational time with the rising of reserved tones,  $L$ . Moreover, we also see that the TR-SE has a computational time of 4.2 s at  $L = 1$  which increases to 16.4 s and 51.3 s at  $L = 2$  and  $L = 3$ , respectively. This is a predictable observation for TR-SE as well since higher numbers of  $L$  result in the higher numbers of search dimensions. Then we see that the CC-TR shows the highest computational time of 44.8 s at just  $L = 1$  for  $I = 200$  iterations which also increases with  $L = 2$ , and  $L = 3$  to 48.6 s and 53.8 s, respectively, just for 1000 OFDM signal samples. This makes the CC-TR difficult to use in real-time transmission of OFDM signals despite having a high PAPR reduction gain. Therefore, we show that our proposed TR-PSO attains a moderately low computational time of 1.0 s with the use of ANNs for  $L = 1,2,3$  canceling signals. Moreover, our proposed TR-PSO also achieves the closest PAPR reduction performance to the CC-TR with  $I = 200$  iterations.

Table 9. Computational time requirements of the PAPR reduction techniques at  $N = 60$  and  $L = 1,2,3$  for 1000 samples

No	Techniques	Computational Time, T (seconds)	Inputs
			$L$
1	TR	6.8	1
		17.9	2
		67.1	3
2	CC-TR ( $I = 200$ )	743.7	1
		750.7	2
		763.3	3
3	SCF	0.7	-
4	TR-SE	16.2	1
		67.8	2
		730.9	3
5	TR-PSO with ANNs	3.0	1
		3.0	2
		3.0	3

Table 10. Computational time requirements of the PAPR reduction techniques at  $N = 124$  and  $L = 1,2,3$  for 50 samples

No	Techniques	Computational Time, T (seconds)	Inputs
			$L$
1	TR	0.4	1
		2.7	2
		18.2	3
2	CC-TR ( $I = 200$ )	156.3	1
		186.9	2
		237.7	3
3	SCF	0.1	-
4	TR-SE	0.9	1
		10.2	2
		232.5	3
5	TR-PSO with ANNs	0.8	1
		0.8	2
		0.8	3

We found similar trends on the experiments for  $N = 60$  and 124 subcarriers (Table 9 and Table 10 respectively). SCF has the lowest computational time at the cost of signal distortion. CC-TR has the best PAPR reduction but its computational time is too high for practical implementation. Our proposed TR-PSO with ANNs can achieve a fair PAPR reduction gain at a reduced computational time even for high number of subcarriers.

## Chapter 6: Conclusion

In this thesis, we have investigated the Tone Reservation (TR) PAPR reduction technique. Our first aim was to find a proper finite set of pre-defined canceling tones for the transmitter to choose from, instead of calculating the optimal values of canceling tones for a given input data as in CC-TR. Particle swarm optimization technique (PSO) is deployed to efficiently search for a good set of canceling tone candidates. In contrast to basic mappings of M-PSK, M-ASK, and M-QAM candidates, a proper and more effective canceling tone candidate set is obtained by the PSO such that PAPR reduction performance is enhanced. These optimized canceling tones are subject to the constraint that the average energy per signal is 1, to ensure that there is no negative effect on the system bit error rate performance. Numerical results reveal that TR with a PSO predefined set of carefully chosen 8 canceling signal candidates provides a fair performance in contrast to the CC-TR and is better than the conventional TR with basic signal mappings.

Moreover, we have also proposed the use of a combination of binary class and multiclass classifiers as a tool on the proposed TR-PSO PAPR reduction technique. To reduce the computational time of TR-PSO ANN is adopted for both tasks. Our proposed TR-PSO with ANNs first applies binary classifier ANN. This ANN module distinguishes OFDM signals in terms of high and low PAPR classes based on a threshold. Then a multiclass ANN classifier is applied on only the high PAPR OFDM signal classes for choosing the appropriate peak canceling signals found from using the TR-PSO technique. Moreover, we also observed that the PAPR reduction performance of our proposed combinations of ANN classifiers with the TR-PSO technique is identical to that of the alternative TR-based full search approach. Therefore, using our proposed combination of ANN classifiers tool reduced the computational times of our proposed TR-PSO PAPR reduction technique by 98% for 60 data subcarriers. Numerical results also show that our proposed binary class and multiclass ANN modules can attain high test accuracies of above 95% when both of them are combined to work cumulatively and automatically. Moreover, we would also like to state that for  $N = 60, 124$  subcarriers the TR-PSO uses the canceling tones that it obtained while minimizing the PAPR of  $N = 13$  subcarriers and it still achieved a fair PAPR reduction gain in contrast to CC-TR with 200 iterations. As a result, the performance of TR-PSO may be improved further in the future by allowing it to learn and adjust its canceling signals from the 60, 124, or higher numbers of subcarriers.

## REFERENCES



จุฬาลงกรณ์มหาวิทยาลัย  
**CHULALONGKORN UNIVERSITY**

- [1] B. Saltzberg, "Performance of an efficient parallel data transmission system," *IEEE Trans. Commun. Technol.*, vol. 15, no. 6, pp. 805–811, 1967, doi: 10.1109/TCOM.1967.1089674.
- [2] L. Wang and C. Tellambura, "A simplified clipping and filtering technique for PAR reduction in OFDM systems," *IEEE Signal Process. Lett.*, vol. 12, no. 6, pp. 453–456, 2005, doi: 10.1109/LSP.2005.847886.
- [3] G. Chen, R. Ansari, and Y. Yao, "Improved peak windowing for PAPR reduction in OFDM," in *VTC Spring 2009 - IEEE 69th Vehicular Technology Conference*, 2009, pp. 1–5, doi: 10.1109/VETECS.2009.5073593.
- [4] X. Huang, J. Lu, J. Zheng, K. B. Letaief, and J. Gu, "Companding transform for reduction in peak-to-average power ratio of OFDM signals," *IEEE Trans. Wirel. Commun.*, vol. 3, no. 6, pp. 2030–2039, 2004, doi: 10.1109/TWC.2004.837619.
- [5] P. Börjesson, H. G. Feichtinger, N. Grip, M. Isaksson, N. Kaiblinger, P. Ödling, and L. Persson, "A low-complexity PAR-reduction method for DMT-VDSL," in *Proc. 5<sup>th</sup> International Symposium on Digital Signal Processing for Communications Systems (DSPCS)*, Perth, Australia, February 1999, pp. 164–169.
- [6] J. Tellado, "Peak to average power ratio reduction for multicarrier modulation," PhD thesis, University of Stanford, Stanford, 1999.
- [7] A. Gatherer and M. Polley, "Controlling clipping probability in DMT transmission," in *Conference Record of the Thirty-First Asilomar Conference on Signals, Systems and Computers (Cat. No.97CB36136)*, 1997, vol. 1, pp. 578–584 vol.1, doi: 10.1109/ACSSC.1997.680443.
- [8] C.-S. Hwang, "A peak power reduction method for multicarrier transmission," *ICC 2001. IEEE International Conference on Communications. Conference Record (Cat. No.01CH37240)*, 2001, pp. 1496–1500 vol.5, doi: 10.1109/ICC.2001.937170.
- [9] R. W. Bäuml, R. F. H. Fischer, and J. B. Huber, "Reducing the peak-to-average power ratio of multicarrier modulation by selected mapping," *Electron. Lett.*, vol. 32, no. 22, pp. 2056–2057, 1996, doi: 10.1049/el:19961384.
- [10] L. J. Cimini and N. R. Sollenberger, "Peak-to-average power ratio reduction of an OFDM signal using partial transmit sequences," *IEEE Commun. Lett.*, vol. 4, no. 3, pp. 86–88, 2000, doi: 10.1109/4234.831033.
- [11] A. D. S. Jayalath and C. Tellambura, "Peak-to-average power ratio reduction of an OFDM signal using data permutation with embedded side information," in *ISCAS 2001. The 2001 IEEE International Symposium on Circuits and Systems (Cat. No.01CH37196)*, 2001, vol. 4, pp. 562–565 vol. 4, doi: 10.1109/ISCAS.2001.922299.
- [12] D. L. Jones, "Peak power reduction in OFDM and DMT via active channel modification," in *Conference Record of the Thirty-Third Asilomar Conference on Signals, Systems, and Computers (Cat. No.CH37020)*, 1999, vol. 2, pp. 1076–1079 vol.2, doi: 10.1109/ACSSC.1999.831875.
- [13] A. Aggarwal and T. H. Meng, "Minimizing the peak-to-average power ratio of OFDM signals using convex optimization," *IEEE Trans. Signal Process.*, vol. 54, no. 8, pp. 3099–3110, 2006, doi: 10.1109/TSP.2006.875390.
- [14] Y. Zhang, A. Yongacoglu, J.-Y. Chouinard, and L. Zhang, "OFDM peak power reduction by sub-block-coding and its extended versions," in *1999 IEEE 49th Vehicular*

- Technology Conference (Cat. No.99CH36363)*, 1999, vol. 1, pp. 695–699 vol.1, doi: 10.1109/VETEC.1999.778254.
- [15] J. A. Davis and J. Jedwab, “Peak-to-mean power control in OFDM, Golay complementary sequences, and Reed-Muller codes,” *IEEE Trans. Inf. Theory*, vol. 45, no. 7, pp. 2397–2417, 1999, doi: 10.1109/18.796380.
- [16] A. A. Abouda, “PAPR reduction of OFDM signal using turbo coding and selective mapping,” in *Proceedings of the 6th Nordic Signal Processing Symposium, 2004. NORSIG 2004.*, 2004, pp. 248–251.
- [17] B. S. Krongold and D. L. Jones, “An active-set approach for OFDM PAR reduction via tone reservation,” *IEEE Trans. Signal Process.*, vol. 52, no. 2, pp. 495–509, 2004, doi: 10.1109/TSP.2003.821110.
- [18] M. Wang, D. E. Quevedo, G. C. Goodwin, and B. S. Krongold, “A complex-baseband active-set approach for tone reservation PAR reduction in OFDM systems,” in *2008 Australian Communications Theory Workshop*, 2008, pp. 113–118, doi: 10.1109/AUSCTW.2008.4460831.
- [19] H. Li, T. Jiang, and Y. Zhou, “An improved tone reservation scheme with fast convergence for PAPR reduction in OFDM systems,” *IEEE Trans. Broadcast.*, vol. 57, no. 4, pp. 902–906, 2011, doi: 10.1109/TBC.2011.2169622.
- [20] F. Tosato, M. Sandell, and M. Tanahashi, “Tone reservation for PAPR reduction: An optimal approach through sphere encoding,” in *2016 IEEE International Conference on Communications (ICC)*, 2016, pp. 1–6, doi: 10.1109/ICC.2016.7511168.
- [21] H. Li, J. Wei, and N. Jin, “Low-complexity tone reservation scheme using pre-generated peak-canceling signals,” *IEEE Commun. Lett.*, vol. 23, no. 9, pp. 1586–1589, 2019, doi: 10.1109/LCOMM.2019.2923617.
- [22] Z. Li, N. Jin, X. Wang, and J. Wei, “Extreme learning machine-based tone reservation scheme for OFDM systems,” *IEEE Wirel. Commun. Lett.*, vol. 10, no. 1, pp. 30–33, Jan. 2021, doi: 10.1109/LWC.2020.3019792.
- [23] S. B. Weinstein, “The history of orthogonal frequency-division multiplexing [history of communications],” *IEEE Commun. Mag.*, vol. 47, no. 11, pp. 26–35, Nov. 2009, doi: 10.1109/MCOM.2009.5307460.
- [24] Y. A. Jawhar *et al.*, “A review of partial transmit sequence for PAPR reduction in the OFDM systems,” *IEEE Access*, vol. 7, pp. 18021–18041, 2019, doi: 10.1109/ACCESS.2019.2894527.
- [25] C. Eklund, R. B. Marks, K. L. Stanwood, and S. Wang, “IEEE standard 802.16: a technical overview of the wirelessMAN/sup TM/air interface for broadband wireless access,” *IEEE communications magazine*, vol. 40, no. 6, pp. 98–107, 2002.
- [26] Y. A. Al-Jawhar, K. N. Ramli, M. A. Taher, N. S. M. Shah, L. Audah, and M. S. Ahmed, “Zero-padding techniques in OFDM systems,” *Int. J. Electr. Eng. Informatics*, vol. 10, no. 4, pp. 704–725, 2018, doi: 10.15676/ijeei.2018.10.4.6.
- [27] I. Sohn and S. C. Kim, “Neural network based simplified clipping and filtering technique for PAPR reduction of OFDM signals,” *IEEE Commun. Lett.*, vol. 19, no. 8, pp. 1438–1441, 2015, doi: 10.1109/LCOMM.2015.2441065.
- [28] D. J. F. Barros, Orthogonal frequency-division multiplexing for optical

communications. Stanford University, 2011.

- [29] M. Janjić and N. Nešković, “A comparative analysis of techniques for PAPR reduction of OFDM signals,” in *2013 21st Telecommunications Forum Telfor (TELFOR)*, 2013, pp. 256–259, doi: 10.1109/TELFOR.2013.6716220.
- [30] W. Strickler, “Using RF power meters for PAPR analysis and reduction,” *Microw. J.*, vol. 62, pp. 80–92, 2019.
- [31] B. Wang, Q. Si, and M. Jin, “A novel tone reservation scheme based on deep learning for PAPR reduction in OFDM systems,” *IEEE Commun. Lett.*, vol. 24, no. 6, pp. 1271–1274, Jun. 2020, doi: 10.1109/LCOMM.2020.2980832.
- [32] J. G. Proakis and D. G. Manolakis, *Digital signal processing, principles, algorithms, and applications*. Englewood Cliffs, NJ: Prentice Hall, 1996.
- [33] L. Li, C. Tellambura, and X. Tang, “Improved tone reservation method based on deep learning for PAPR reduction in OFDM system,” in *2019 11th International Conference on Wireless Communications and Signal Processing (WCSP)*, Oct. 2019, pp. 1–6, doi: 10.1109/WCSP.2019.8928103.
- [34] S. H. Han and J. H. Lee, “An overview of peak-to-average power ratio reduction techniques for multicarrier transmission,” *IEEE Wirel. Commun.*, vol. 12, no. 2, pp. 56–65, 2005, doi: 10.1109/MWC.2005.1421929.
- [35] T. Jiang and Y. Wu, “An overview: peak-to-average power ratio reduction techniques for OFDM signals,” *IEEE Trans. Broadcast.*, vol. 54, no. 2, pp. 257–268, 2008, doi: 10.1109/TBC.2008.915770.
- [36] G. Wunder, R. F. H. Fischer, H. Boche, S. Litsyn, and J.-S. No, “The PAPR problem in OFDM transmission: new directions for a long-lasting problem,” *IEEE Signal Process. Mag.*, vol. 30, no. 6, pp. 130–144, Nov. 2013, doi: 10.1109/msp.2012.2218138.
- [37] J. Armstrong, “Peak-to-average reduction for OFDM by repeated clipping and frequency domain filtering,” *Electron. Lett.*, vol. 38, pp. 246–247, 2002, doi: 10.1049/el:20020175.
- [38] Y.-C. Wang and Z.-Q. Luo, “Optimized iterative clipping and filtering for PAPR reduction of OFDM signals,” *IEEE Trans. Commun.*, vol. 59, no. 1, pp. 33–37, 2011, doi: 10.1109/TCOMM.2010.102910.090040.
- [39] J. Kennedy and R. Eberhart, “Particle swarm optimization,” in *Proceedings of ICNN'95 - International Conference on Neural Networks*, 1995, vol. 4, pp. 1942–1948 vol.4, doi: 10.1109/ICNN.1995.488968.
- [40] R. Al Ahsan and L. Wuttisittikulij, “Artificial neural network (ANN) based classification of high and low PAPR OFDM signals,” in *2021 36th International Technical Conference on Circuits/Systems, Computers and Communications (ITC-CSCC)*, 2021, pp. 1–4, doi: 10.1109/ITC-CSCC52171.2021.9501484.



## VITA

**NAME** Rafee Al Ahsan

**DATE OF BIRTH** 17 March 1997

**PLACE OF BIRTH** Dhaka, Bangladesh

**INSTITUTIONS ATTENDED** Ahsanullah University of Science and Technology, (AUST)

**HOME ADDRESS** 13/1 Free School Street Kathalbagan, Dhaka, 1205, Bangladesh

**PUBLICATION** R. Al Ahsan and L. Wuttisittikulkij, “Artificial Neural Network (ANN) based Classification of High and Low PAPR OFDM signals,” in 2021 36th International Technical Conference on Circuits/Systems, Computers and Communications (ITC-CSCC), 2021, pp. 1–4, doi: 10.1109/ITC-CSCC52171.2021.9501484.

**AWARD RECEIVED** ASEAN and NON-ASEAN SCHOLARSHIP